Angewandte Chemie
Eine Zeitschrift der Gesellschaft Deutscher Chemiker

Supporting Information

Separating Dipolar and Chemical Exchange Magnetization Transfer Processes in ^{1}H-CEST

*Tairan Yuwen, Ashok Sekhar, and Lewis E. Kay**

anie_201610759_sm_miscellaneous_information.pdf

Supporting Information

Table of Contents

Materials and Methods

Details of the amide ^{1}H-CEST, TROSY-based, spin-state selective pulse scheme of Figure 2. 90° (180°) rectangular pulses, denoted by narrow (wide) black rectangles, are applied at maximum power for ^{1}H and ^{15}N. Water-selective rectangular pulses typically have durations of 1.7–1.8 ms. The ^{1}H carrier is set at the water resonance, while the ^{15}N carrier is placed at the center of the amide ^{15}N spectral region, ∼119 ppm. The delays used are: $\tau_a \simeq \tau_b \simeq 1/(4^1J_{NH}) = 2.70$ ms, $\Delta = 850\ \mu s$, $\delta = 500\ \mu s$. All pulses are applied with phase x unless otherwise indicated. The following phase cycle is used: $\phi_2 = y,-y,-x,x$; $\phi_3 = y$; $\phi_4 = -y$; $\phi_5 = -y$; $\phi_{\rm rec} = -y,y,-x,x$. Quadrature detection in F_1 is achieved by inverting the phases of $\phi_3, \phi_4, \phi_5, \phi_{\rm rec}$ together with the sign of gradient g_9[1], and changing ϕ_2 to $y,-y,x,-x$. A minimum 4 step cycle is recommended for optimal TROSY selection, however two steps is sufficient since coherence selection gradients (g_6, g_9) are applied. Two CEST profiles, corresponding to selection of $IN^{I\alpha}$ and $IN^{I\beta}$ pathways are collected by setting ϕ_1 to $-x$ or x, respectively and storing the resulting datasets in separate memory locations. Gradients are applied with the following durations (ms) and strengths (in % maximum): g_1: (0.4, −25%), g_2: (1.0, 15%), g_3: (0.5, −50%), g_4: (0.256, 23%), g_5: (1.5, −70%), g_6: (0.625, 80%), g_7: (0.256, 60%), g_8: (0.256, 15%), g_9: (0.256, −39.5%). The gradient strengths g_7 and g_8 are chosen according to Mulder et al.[2] in order to minimize weak F_2 phasing artifacts. The weak ^{1}H B_1 field was calibrated using the approach of Guenneugues et al.[3]

Sample preparation. An NMR sample of [U-^{2}H; Ileδ1-^{13}CHD$_2$; Leu,Val-^{13}CHD$_2$/^{13}CHD$_2$; Met-^{13}CHD$_2$] G48A Fyn SH3 was prepared as described previously[4], with 1.35 mM protein dissolved in 50 mM sodium phosphate, 0.2 mM EDTA, 0.05% NaN_3, pH 7.0, 90%H_2O/10%D_2O (note that methyl labeling is not required for this experiment). A 1.5 mM U-[^{15}N, ^{2}H] L99A T4L sample was generated following the protocol described by Bouvignies et al.[5]; buffer conditions are 50 mM sodium phosphate, 25 mM NaCl, 2 mM EDTA, 2 mM NaN_3, pH 5.5, 90%H_2O/10%D_2O.

NMR spectroscopy. ^{1}H and ^{15}N CEST datasets were recorded on G48A Fyn SH3 using a 600 MHz Bruker spectrometer equipped with a triple-axis cryogenically cooled probe, 11°C. ^{15}N CEST datasets were collected using the standard pulse scheme as described previously[6] with three different weak B_1 fields (13.5, 22.8 and 36.4 Hz) and T_{Ex} = 400 ms. A pair of ^{1}H CEST datasets was recorded with the pulse scheme of Figure S1 using B_1 fields of 26.7 Hz and 42.0 Hz. A value of T_{Ex} = 400 ms was chosen. Experiments were obtained as interleaved pseudo-4D datasets by recording a pair of components that are then manipulated to separate $IN^{I\alpha}$ and $IN^{I\beta}$ pathways (see Figure S1) and by varying the position of the weak ^{1}H CEST field during T_{Ex} for each 2D spectrum (over the range of 5.5–10.5 ppm) with step sizes of 25 Hz ($B_1 \sim 25$ Hz) or 40 Hz ($B_1 \sim 40$ Hz). In addition a 2D reference dataset was recorded with a B_1 offset of -12 kHz that is equivalent to setting $B_1 = 0$ Hz. This dataset was used to rescale the CEST baseline to 1 for each profile (see below). Each 2D dataset was recorded with 2 transients/FID, a relaxation delay of 1.5 s and (640, 32) complex points in (t_2, t_1) to give a net acquisition time of ∼4 min/spectrum. The net measurement time for each CEST dataset was ∼16 h ($B_1 \sim 25$ Hz) or ∼10 h ($B_1 \sim 40$ Hz).

^{1}H and ^{15}N CEST experiments were measured for L99A T4L using an 800 MHz Bruker spectrometer equipped with a z-axis cryogenically cooled probe. ^{1}H experiments were recorded with the scheme of Figure 2 and the standard ^{15}N-CEST pulse sequence[6] was used for measurement of ^{15}N datasets. ^{1}H-CEST measurements were performed with weak B_1 fields of 30.5 Hz (8.8°C) or 30.7 Hz (13.5°C), T_{Ex} = 400 ms. Experiments were recorded as pseudo-4D datasets by recoding pairs of interleaved spectra derived from $IN^{I\alpha}$ and $IN^{I\beta}$ magnetization transfer pathways and by varying the position of the ^{1}H offset during T_{Ex} after each pair of 2D spin-state selective spectra were obtained. A range of ^{1}H offsets from 6.5–9.5 ppm was chosen, with step sizes of 30 Hz. An additional reference 2D dataset was obtained by setting the B_1 offset to -12 kHz. Each 2D dataset was recorded with 4 transients/FID, a relaxation delay of 1.5 s and (768, 64) complex points in (t_2, t_1) to give a net acquisition time of ∼15 min/spectrum. The total measurement time for each pseudo-4D was ∼48 h.

Data analysis. All NMR spectra were processed and analyzed using the NMRPipe suite of programs[7]. Analysis of CEST profiles was carried out using the software package ChemEx (https://github.com/gbouvignies/chemex); a separate module is required for fitting the difference ^{1}H-CEST profiles, $IN^{I\beta} - IN^{I\alpha}$, which is available upon request. Prior to the calculation of the difference ^{1}H-CEST profile each of the $IN^{I\alpha}$ and $IN^{I\beta}$ CEST curves was first rescaled to bring the baseline position to 1.0. This is achieved by measuring a reference plane with the full CEST duration but without the weak B_1 field, $I(T_{Ex}, B_1 = 0)$ or alternatively, by placing B_1 far off-resonance, (e.g. -12000 Hz), as described above. The ratio $I(T_{Ex}, B_1)/I(T_{Ex}, B_1 = 0)$ is then plotted as a function of the position of the weak B_1 field which automatically produces rescaled CEST profiles. Note that the effects of rescaling are very minimal. Differences in CEST baselines for profiles derived from $IN^{I\alpha}$ and $IN^{I\beta}$ pathways result from ^{1}H–^{15}N dipolar/^{1}H CSA cross-correlated relaxation. These effects are very small since they scale as $1/\omega_H^2$ in the macromolecular limit[8]. For example, we have measured average differences in R_1 rates for $I_z N^{I\alpha}$ and $I_z N^{I\beta}$ of 0.02 ± 0.05 s^{-1} (11°C, 600 MHz) and 0.01 ± 0.03 s^{-1} (9°C, 800 MHz) for the amide protons of Fyn SH3 and L99A T4L, respectively. Exchange parameters were extracted from global fits of CEST profiles to a two-site exchange model using the Bloch–McConnell equations[9], as described below. In total 46 and 62 CEST profiles were selected for G48A Fyn SH3 and L99A T4L, respectively, to extract $\Delta\varpi_{GE}$ values. For G48A Fyn SH3, only those CEST profiles (30 residues) with distinct minor and major dips were chosen to estimate (p_E, k_{ex}), while for L99A T4L reliable exchange parameters, (p_E, k_{ex}), could not be obtained because of ^{1}H–^{1}H cross-relaxation effects (see text and below).

CEST profiles were fit to a model of exchange, $G \underset{k_{EG}}{\overset{k_{GE}}{\rightleftharpoons}} E$, where the evolution of an isolated scalar-coupled ^{1}H$^{\mathrm{N}}$–^{15}N spin system was considered as follows

$$\frac{d}{dt}\mathbf{m}(t) = \mathbf{L} \cdot \mathbf{m}(t). \qquad \text{[S1]}$$

In Eq. [S1] $\mathbf{m}$ is a 13×1 column vector with the first (second) 6 rows comprising

density elements for state G (E) and the last element, Z, the identity operator,

$$\mathbf{m} = (H_x^G, H_y^G, H_z^G, 2H_x^G N_z^G, 2H_y^G N_z^G, 2H_z^G N_z^G, H_x^E, H_y^E, H_z^E, 2H_x^E N_z^E, 2H_y^E N_z^E, 2H_z^E N_z^E, Z)^T \qquad \text{[S2]}$$

where H_i^j and N_i^j denote ^{1}H$^{\mathrm{N}}$ and ^{15}N magnetization elements, respectively, $i \in \{x,y,z\}$, $j \in \{G,E\}$ and 'T' is the transpose operator. The matrix $\mathbf{L}$ is given by[10,11]

$$\mathbf{L} = -\left[\begin{array}{cccccc:cccccc:c}
R_{Hxy}^G + k_{GE} & \omega_H^G & 0 & \eta_{Hxy}^G & \pi J_{HN}^G & 0 & -k_{EG} & 0 & 0 & 0 & 0 & 0 & 0 \\
-\omega_H^G & R_{Hxy}^G + k_{GE} & \omega_{1H} & -\pi J_{HN}^G & \eta_{Hxy}^G & 0 & 0 & -k_{EG} & 0 & 0 & 0 & 0 & 0 \\
0 & -\omega_{1H} & R_{Hz}^G + k_{GE} & 0 & 0 & \eta_{Hz}^G & 0 & 0 & -k_{EG} & 0 & 0 & 0 & \Theta^G \\
\eta_{Hxy}^G & \pi J_{HN}^G & 0 & R_{2HxyNz}^G + k_{GE} & \omega_H^G & 0 & 0 & 0 & 0 & -k_{EG} & 0 & 0 & 0 \\
-\pi J_{HN}^G & \eta_{Hxy}^G & 0 & -\omega_H^G & R_{2HxyNz}^G + k_{GE} & \omega_{1H} & 0 & 0 & 0 & 0 & -k_{EG} & 0 & 0 \\
0 & 0 & \eta_{Hz}^G & 0 & -\omega_{1H} & R_{2HzNz}^G + k_{GE} & 0 & 0 & 0 & 0 & 0 & -k_{EG} & 0 \\
\hdashline
-k_{GE} & 0 & 0 & 0 & 0 & 0 & R_{Hxy}^E + k_{EG} & \omega_H^E & 0 & \eta_{Hxy}^E & \pi J_{HN}^E & 0 & 0 \\
0 & -k_{GE} & 0 & 0 & 0 & 0 & -\omega_H^E & R_{Hxy}^E + k_{EG} & \omega_{1H} & -\pi J_{HN}^E & \eta_{Hxy}^E & 0 & 0 \\
0 & 0 & -k_{GE} & 0 & 0 & 0 & 0 & -\omega_{1H} & R_{Hz}^i + k_{EG} & 0 & 0 & \eta_{Hz}^E & \Theta^E \\
0 & 0 & 0 & -k_{GE} & 0 & 0 & \eta_{Hxy}^E & \pi J_{HN}^E & 0 & R_{2HxyNz}^E + k_{EG} & \omega_H^E & 0 & 0 \\
0 & 0 & 0 & 0 & -k_{GE} & 0 & -\pi J_{HN}^E & \eta_{Hxy}^E & 0 & -\omega_H^E & R_{2HxyNz}^E + k_{EG} & \omega_{1H} & 0 \\
0 & 0 & 0 & 0 & 0 & -k_{GE} & 0 & 0 & \eta_{Hz}^E & 0 & -\omega_{1H} & R_{2HzNz}^E + k_{EG} & 0 \\
\hdashline
0 & 0 & 0 & 0 & 0 & 0 & 0 & 0 & 0 & 0 & 0 & 0 & 0
\end{array}\right] \qquad \text{[S3]}$$

where R_{Hxy}^j (R_{2HxyNz}^j) is the ^{1}H$^{\mathrm{N}}$ in-phase (anti-phase) transverse relaxation rate (s^{-1}), R_{Hz}^j is the ^{1}H$^{\mathrm{N}}$ longitudinal relaxation rate (s^{-1}), R_{2HzNz}^j is the relaxation rate of longitudinal two-spin order, η_{Hxy}^j (η_{Hz}^j) is the ^{1}H$^{\mathrm{N}}$ transverse (longitudinal) dipole–CSA cross-correlation relaxation rate, ω_H^j is the offset (in rad/s) of the ^{1}H$^{\mathrm{N}}$ resonance from the position of the weak CEST field of strength ω_{1H} (ω_H^G is obtained from the ground-state peak position and is not a fitting parameter), and J_{HN}^j is the ^{1}H$^{\mathrm{N}}$–^{15}N scalar coupling constant (fixed to -93 Hz). The parameters Θ^G, Θ^E are defined as follows $\Theta^G = -R_{Hz}^G H_o^G, \Theta^E = -R_{Hz}^E H_o^E$ where H_o is the equilibrium value of longitudinal magnetization. In order to simplify the fitting procedure the following relations have been used[10]

$$R_{Hz}^G \simeq R_{Hz}^E,\ R_{2HzNz}^G \simeq R_{2HzNz}^E \simeq R_{Hz}^G + R_{Nz}^G,\ R_{2HxyNz}^G \simeq R_{Hxy}^G - R_{Nz}^G. \qquad \text{[S4]}$$

Assuming that the relative magnitude of H_o^G is 1 the initial boundary conditions become $\mathbf{m}(0) = (0,0,\kappa,0,0,0,0,0,\kappa p_E/(1-p_E),0,0,0,1)^T$; the difference CEST profile is given by the magnitude of the sixth element of $\mathbf{m}(T_{Ex})$. The parameter κ is the fraction

of the equilibrium magnetization that is present at the beginning of the CEST period, which can be calculated as $\kappa = 1 - e^{-R_{Hz}(RD+ATt_2)}$ where RD and ATt_2 are the relaxation delay between scans and the acquisition time in the direct dimension, respectively. Fitting parameters include $R^G_{Hxy}, R^E_{Hxy}, \eta^G_{Hxy}, \eta^E_{Hxy}, R^G_{Nz}, \omega^E_H, p_E, k_{ex}$, with ω^G_H, πJ^G_{HN} and πJ^E_{HN} fixed. The parameter $R^G_{Hz} (\simeq R^E_{Hz})$ can be easily measured from the buildup curve of H_z magnetization (see enclosed pulse sequence code) or, alternatively, treated as a fitting parameter. Both approaches produce essentially identical fitted (p_E, k_{ex}) values for Fyn SH3. In order to minimize the number of fitting parameters and reduce fitting uncertainties, it is assumed that $\eta^G_{Hz} = \eta^E_{Hz} = 0$ since the baseline rescaling procedure largely suppresses this effect. In any event η_{Hz} values are very small, typically on the order of 0.01 s^{-1} for the proteins considered here (see previous section). As described briefly in the text and in detail below, in general, the exchange parameters (p_E, k_{ex}) cannot be well determined from ^{1}H-CEST because of cross-relaxation between adjacent protons. Thus, all parameters above can be considered residue specific in the analysis (p_E values will vary on a per-residue basis in a manner that depends on the proton density surrounding the site of interest). In cases involving applications to highly deuterated small proteins, such as the Fyn SH3 domain (7 kDa) where cross-relaxation rates are small (and not included in the above expressions, see below), it is possible to obtain accurate (p_E, k_{ex}) values; in this case p_E and k_{ex} are global parameters. In general, exchange parameters are best obtained via ^{15}N- or ^{13}C-CEST experiments where the effects of cross-relaxation are not an issue. It is noteworthy that setting (p_E, k_{ex}) as residue-specific in analyses does not affect the robustness of the extracted chemical shifts of the excited state as these are determined from the position of the minor state dip. The fitting procedure described above has been implemented in the ChemEx program as a separate module and is available upon request. In all of the data analyses we have used a value of -93 Hz for $J^G_{HN} (= J^E_{HN})$. Simulations of CEST profiles for a range of $J^G_{HN} (= J^E_{HN})$ between -90 and -96 Hz that are then fitted with a fixed value of $J^G_{HN} (= J^E_{HN}) = -93$ Hz show that $\Delta\varpi_{GE}$ values differ from input chemical shift differences by less than 0.01 ppm at 600 MHz.

Effects of ^{1}H cross-relaxation and ^{15}N spin relaxation on intensities of CEST dips and robustness of extracted exchange parameters (p_E, k_{ex}). As discussed in the text, the presence of a multitude of ^{1}H–^{1}H cross-relaxation pathways in a protein adversely affects the size of the resulting ^{1}H-CEST dips. In the discussion that follows below we provide an intuitive feel for how this comes about by considering a set of simplified equations that describes chemical exchange of a ^{1}H spin of interest in a large 'bath' of surrounding protons. For simplicity we neglect the attached ^{15}N. Subsequently we reintroduce the ^{15}N spin and consider how ^{15}N longitudinal relaxation influences the size of CEST profiles as well. Of course, in experimental applications, and in simulations, both of these effects discussed individually, are operative simultaneously.

(i) Effects of ^{1}H cross-relaxation on CEST dip sizes. In the discussion that follows we assume that the CEST and NOE dips well separated. Placement of the weak B_1 field at the resonance frequency of the excited state spin leads to a decrease in longitudinal ground state ^{1}H magnetization (CEST effect) that, in turn, is replenished from cross-relaxation with neighboring ^{1}H spins. The excited state dip is thus smaller than expected, although the linewidth is little affected, leading to a larger impact on p_E than k_{ex}, with the fitted p_E value underestimated. This can be understood more quantitatively using the Solomon equations that describe the evolution of ^{1}H longitudinal magnetization[8]. In what follows we consider an I spin of interest that undergoes exchange between states G and E as well as a large set of N spins, S^i, that are dipolar coupled to spin I. Neglecting exchange for the moment we can write

$$\begin{aligned} \frac{dI_z}{dt} &= -\rho_I(I_z - I_o) - \sigma_{SI}\sum_{i=1}^{N}(S_z^i - S_o^i) \\ \frac{dS_z^i}{dt} &= -\rho_S(S_z^i - S_o^i) - \sigma_{IS}(I_z - I_o) \end{aligned} \qquad \text{[S5]}$$

where ρ and $\sigma_{SI} = \sigma_{IS}$ are auto- and cross-relaxation rates defined in the usual way[8], all S^i spins are assumed to have the same ρ value and we have written only the equation

describing the evolution of S_z^i for simplicity. Summing over all N S^i spins yields

$$\begin{aligned}\frac{dI_z}{dt} &= -\rho_I(I_z - I_o) - \sigma_{SI}(S_z^{SS} - S_o^{SS}) \\ \frac{dS_z^{SS}}{dt} &= -\rho_S(S_z^{SS} - S_o^{SS}) - N\sigma_{IS}(I_z - I_o)\end{aligned} \qquad [S6]$$

where super-spin S^{SS} is defined as $S_z^{SS} = \sum_{i=1}^{N} S_z^i$. The values of ρ_I and ρ_S are given by

$$\begin{aligned}\rho_I &= \rho_{I,o} - \sigma \\ \rho_S &= \rho_{S,o} - \frac{\sigma}{N}\end{aligned} \qquad [S7]$$

where $\sigma_{SI} = \sigma_{IS} = \frac{\sigma}{N}$, ρ_o includes spectral density terms evaluated at $\omega = \omega_H$ and $\omega = 2\omega_H$, while in the macromolecular limit considered here σ is proportional to a spectral density term at $\omega = 0$ so that $-\sigma \gg \rho_o$ (σ is negative). Finally, because N is large we assume that any perturbation to spin I, such as that introduced through application of a CEST B_1 field on resonance with either ground or excited state spins I, will not affect spin S^{SS}. Thus, to a good approximation $(S_z^{SS} - S_o^{SS})/S_o^{SS} \approx 0$ for the duration of the CEST period. This assumption leads to a rather simple time evolution of I_z

$$\frac{dI_z^G}{dt} = -\rho_I(I_z^G - I_o^G) - k_{GE}I_z^G + k_{EG}I_z^E \qquad [S8]$$

that includes chemical exchange, where superscripts G and E delineate spins in each of the interconverting states.

The CEST profile for spin I is generated by applying a weak ^{1}H B_1 field across the spectrum of ^{1}H chemical shifts and recording I_z^G at each position. In what follows we assume that I and the 'bath' spins S^i are non-degenerate. When the B_1 field is at the resonance position of the excited state for spin I, and assuming that $\omega_1 \gg k_{EG}$, Eq. [S8] becomes

$$\frac{dI_z^G}{dt} = -(\rho_I + k_{GE})(I_z^G - \frac{\rho_I}{\rho_I + k_{GE}}I_o^G) \qquad [S9]$$

so that

$$\frac{I_z^G(T)}{I_o^G} = \frac{\rho_I}{\rho_I + k_{GE}} + \frac{k_{GE}}{\rho_I + k_{GE}} \exp(-(\rho_I + k_{GE})T). \qquad [S10]$$

Eq. [S10] assumes that $I_z^G(0) = I_o^G$. In contrast, when the B_1 field is applied off-resonance from any of the spins then $I_z^G(T) = I_o^G$ that defines the baseline of the CEST profile. The size of the minor state CEST dip is given by the difference in $I_z^G(T)$ values when the B_1 field is off/on resonance,

$$I^{CEST} = I_o^G \frac{k_{GE}}{\rho_I + k_{GE}} (1 - \exp(-(\rho_I + k_{GE})T)). \qquad [S11]$$

In the limit when $\sigma \to 0$ (*i.e.*, no cross-relaxation) then $\rho_I \to \rho_{I,o}$ and

$$I^{CEST}(\sigma \to 0) = I_o^G \frac{k_{GE}}{\rho_{I,o} + k_{GE}} (1 - \exp(-(\rho_{I,o} + k_{GE})T)). \qquad [S12]$$

Since $-\sigma \gg \rho_o$, it follows that $\rho_I \gg \rho_{I,o}$ and numerical simulations show that $I^{CEST}(\sigma \to 0) \geq I^{CEST}$, Figure S2, with equality only for $T \sim 0$.

(ii) Effects of ^{15}N longitudinal relaxation. In what follows we neglect ^{1}H cross-relaxation and consider only a ^{1}H spin, I, one bond coupled to its attached ^{15}N. Relaxation of I magnetization during the CEST delay can then be expressed as

$$\begin{aligned} \frac{dI_z}{dt} &= -\rho_{IP} I_z \\ \frac{d2I_zN_z}{dt} &= -\rho_{AP} 2I_zN_z \end{aligned} \qquad [S13]$$

where ρ_{IP} and ρ_{AP} are the relaxation rates of I longitudinal magnetization and two-spin order, respectively. It is readily shown that even for small proteins at moderate static magnetic fields $\rho_{AP} - \rho_{IP} \approx T_{1N}^{-1}$ where T_{1N}^{-1} is the ^{15}N longitudinal relaxation rate so that Eq. [S13] can be written in terms of single-spin basis operators as follows,

$$\frac{d}{dt} \begin{bmatrix} I_zN^\alpha \\ I_zN^\beta \end{bmatrix} = - \begin{bmatrix} \rho_{IP} + \frac{T_{1N}^{-1}}{2} & -\frac{T_{1N}^{-1}}{2} \\ -\frac{T_{1N}^{-1}}{2} & \rho_{IP} + \frac{T_{1N}^{-1}}{2} \end{bmatrix} \begin{bmatrix} I_zN^\alpha \\ I_zN^\beta \end{bmatrix}. \qquad [S14]$$

Eq. [S14] does not include the effects of cross-correlated spin relaxation involving ^{1}H–^{15}N dipolar/^{1}H chemical shift anisotropy interactions, but these are small as discussed above. ^{15}N relaxation during the CEST element thus leads to mixing of the I_zN^α and I_zN^β magnetization components, resulting in additional dips in ^{1}H CEST profiles (before generating the difference CEST profile). For example, if $T_{1N}^{-1} = 0$ the $IN^{I\alpha}$ profile has major and minor dips at $\omega_I^G - \pi J_{HN}$ and $\omega_I^E - \pi J_{HN}$, respectively ($J_{HN} < 0$). In contrast, when mixing occurs a second set of smaller 'shoulder' dips appears at $\omega_I^G + \pi J_{HN}$ and $\omega_I^E + \pi J_{HN}$. A similar situation occurs for the $IN^{I\beta}$ path, with major and minor dips at $\omega_I^G + \pi J_{HN}$ and $\omega_I^E + \pi J_{HN}$, respectively, in the absence of ^{15}N spin relaxation, and with additional smaller dips at $\omega_I^G - \pi J_{HN}$ and $\omega_I^E - \pi J_{HN}$ when $T_{1N}^{-1} \neq 0$. Thus when the difference CEST profile is generated the 'shoulder' dips subtract from the main dips (both for the ground and excited states). The net effect is that dips in the difference CEST profiles are reduced.

Figure S3 shows results from numerical simulations that include both of the effects described above. The computations were based on the Bloch–McConnell equations (see Eq. [S16] below) with a basis that includes, in addition to the 13 elements in Eq. [S2], also S_z^{SS} and $2S_z^{SS}N_z$ that couple to the previous basis elements via Eq. [S6] and an additional pair of equations

$$\begin{aligned} \frac{d2I_zN_z}{dt} &= -\rho_I 2I_zN_z - \frac{\sigma}{N} 2S_z^{SS}N_z \\ \frac{d2S_z^{SS}N_z}{dt} &= -\rho_S 2S_z^{SS}N_z - \sigma 2I_zN_z. \end{aligned} \qquad [S15]$$

The resulting Bloch–McConnell equation becomes

$$\frac{d}{dt}\begin{bmatrix} H_x^G \\ H_y^G \\ H_z^G \\ 2H_x^G N_z^G \\ 2H_y^G N_z^G \\ 2H_z^G N_z^G \\ H_x^E \\ H_y^E \\ H_z^E \\ 2H_x^E N_z^E \\ 2H_y^E N_z^E \\ 2H_z^E N_z^E \\ S_z^{SS} \\ 2S_z^{SS} N_z^G \\ Z \end{bmatrix} = -\left[\begin{array}{cccccc:cccccc:ccc:c} R_{Hxy}^G + k_{GE} & \omega_H^G & 0 & \eta_{Hxy}^G & \pi J_{HN}^G & 0 & -k_{EG} & 0 & 0 & 0 & 0 & 0 & 0 & 0 & 0 & H_x^G \\ -\omega_H^G & R_{Hxy}^G + k_{GE} & \omega_{1H} & -\pi J_{HN}^G & \eta_{Hxy}^G & 0 & 0 & -k_{EG} & 0 & 0 & 0 & 0 & 0 & 0 & 0 & H_y^G \\ 0 & -\omega_{1H} & R_{Hz}^G + k_{GE} & 0 & 0 & \eta_{Hz}^G & 0 & 0 & -k_{EG} & 0 & 0 & 0 & \sigma/N & 0 & \Theta_I^G & H_z^G \\ \eta_{Hxy}^G & \pi J_{HN}^G & 0 & R_{2HxyNz}^G + k_{GE} & \omega_H^G & 0 & 0 & 0 & 0 & -k_{EG} & 0 & 0 & 0 & 0 & 0 & 2H_x^G N_z^G \\ -\pi J_{HN}^G & \eta_{Hxy}^G & 0 & -\omega_H^G & R_{2HxyNz}^G + k_{GE} & \omega_{1H} & 0 & 0 & 0 & 0 & -k_{EG} & 0 & 0 & 0 & 0 & 2H_y^G N_z^G \\ 0 & 0 & \eta_{Hz}^G & 0 & -\omega_{1H} & R_{2HzNz}^G + k_{GE} & 0 & 0 & 0 & 0 & 0 & -k_{EG} & 0 & \sigma/N & 0 & 2H_z^G N_z^G \\ \hdashline -k_{GE} & 0 & 0 & 0 & 0 & 0 & R_{Hxy}^E + k_{EG} & \omega_H^E & 0 & \eta_{Hxy}^E & \pi J_{HN}^E & 0 & 0 & 0 & 0 & H_x^E \\ 0 & -k_{GE} & 0 & 0 & 0 & 0 & -\omega_H^E & R_{Hxy}^E + k_{EG} & \omega_{1H} & -\pi J_{HN}^E & \eta_{Hxy}^E & 0 & 0 & 0 & 0 & H_y^E \\ 0 & 0 & -k_{GE} & 0 & 0 & 0 & 0 & -\omega_{1H} & R_{Hz}^E + k_{EG} & 0 & 0 & \eta_{Hz}^E & 0 & 0 & \Theta_I^E & H_z^E \\ 0 & 0 & 0 & -k_{GE} & 0 & 0 & \eta_{Hxy}^E & \pi J_{HN}^E & 0 & R_{2HxyNz}^E + k_{EG} & \omega_H^E & 0 & 0 & 0 & 0 & 2H_x^E N_z^E \\ 0 & 0 & 0 & 0 & -k_{GE} & 0 & -\pi J_{HN}^E & \eta_{Hxy}^E & 0 & -\omega_H^E & R_{2HxyNz}^E + k_{EG} & \omega_{1H} & 0 & 0 & 0 & 2H_y^E N_z^E \\ 0 & 0 & 0 & 0 & 0 & -k_{GE} & 0 & 0 & \eta_{Hz}^E & 0 & -\omega_{1H} & R_{2HzNz}^E + k_{EG} & 0 & 0 & 0 & 2H_z^E N_z^E \\ \hdashline 0 & 0 & \sigma & 0 & 0 & 0 & 0 & 0 & 0 & 0 & 0 & 0 & R_{Hz}^S & 0 & \Theta_S & S_z^{SS} \\ 0 & 0 & 0 & 0 & 0 & \sigma & 0 & 0 & 0 & 0 & 0 & 0 & 0 & R_{2HzNz}^S & 0 & 2S_z^{SS} N_z^G \\ \hdashline 0 & 0 & 0 & 0 & 0 & 0 & 0 & 0 & 0 & 0 & 0 & 0 & 0 & 0 & 0 & Z \end{array}\right]\begin{bmatrix} H_x^G \\ H_y^G \\ H_z^G \\ 2H_x^G N_z^G \\ 2H_y^G N_z^G \\ 2H_z^G N_z^G \\ H_x^E \\ H_y^E \\ H_z^E \\ 2H_x^E N_z^E \\ 2H_y^E N_z^E \\ 2H_z^E N_z^E \\ S_z^{SS} \\ 2S_z^{SS} N_z^G \\ Z \end{bmatrix}$$

[S16]

where $\Theta_I^G = -R_{Hz}^G H_o^G - \dfrac{\sigma}{N} S_o^{SS}, \Theta_I^E = -R_{Hz}^E H_o^E, \Theta_S = -R_{Hz}^S S_o^{SS} - \sigma H_o^G$ account for the relaxation of longitudinal H and S^{SS} magnetization back to their equilibrium values, H_o^G and S_o^{SS}, respectively and R_{Hz}^G (R_{Sz}) in Eq. [S16] is identified with $\rho_{I,o}$ ($\rho_{S,o}$) in Eqs [S6] and [S15]. In the above discussion we have neglected cross-relaxation in the excited state. Further, assuming that the magnitude of H_o^G is 1, then the initial boundary condition becomes $\mathbf{m}(0) = (0,0,\kappa,0,0,0,0,0,\kappa p_E/(1-p_E),0,0,0,\kappa S_o^{SS}/H_o^G,0,1)^T$ with the difference CEST profile given by the magnitude of the sixth element of $\mathbf{m}(T_{Ex})$ and κ is the fraction of the equilibrium magnetization that is present at the beginning of CEST period (see above). In all of the simulation we have assumed that $\eta_{Hz}^G = \eta_{Hz}^E = 0$, $R_{Hz} = 0\ \mathrm{s}^{-1}$, $\kappa = 1$, $N = 100$ and $S_o^{SS} = N \times H_o^G$. Also shown in Figure S3 are histograms of measured values of ρ_N and σ for L99A T4L, 9°C, as well of plots that calculate how these values vary with molecular tumbling time.

The above discussion makes it clear that both ^{1}H and ^{15}N relaxation lead to decreases in the sizes of the resulting CEST dips in difference profiles. It is difficult to account rigorously for ^{1}H cross-relaxation so that in general robust values of exchange parameters (p_E, k_{ex}) will not be obtained via this method, yet accurate ^{1}H $\Delta\varpi$ values are readily fit.

Optimal choice of B_1 field strengths in CEST measurements. In order to optimize signal-to-noise in CEST profiles (*i.e.*, large dips) it is necessary to choose weak B_1 fields judiciously. This is particularly important in the context of the ^{1}H-CEST experiments considered here where the line-shapes of the difference CEST profiles used in analyses can be approximated as anti-phase absorptive (see below), leading to attenuation of dips if larger than optimal values of B_1 are selected. Zaiss and Bachert have derived a set of equations that enable an evaluation of the sizes of CEST dips for a given set of exchange parameters and a fixed CEST B_1 field[12]. Noting that CEST experiments, in general, are analogous to $R_{1\rho}$ measurements with a weak B_1 field, the decay rate of magnetization for spin I from the ground state is given by[12]

$$R_{1\rho}(\Delta\omega) = R_{eff}(\Delta\omega) + R_{ex}(\Delta\omega) \qquad \text{[S17]}$$

where $R_{eff}(\Delta\omega)$ is the intrinsic relaxation of spin I as a function of the offset between the B_1 field and the resonance position of the spin ($\Delta\omega$, rad/s) and $R_{ex}(\Delta\omega)$ is the contribution to the relaxation of I from the exchange process. In what follows it is convenient to recast Eq. [S17] in terms of the offset of the weak B_1 CEST field relative to the resonance position of the excited state spin, $\Delta\omega_E$. In the limit that longitudinal relaxation rates for spins in G and E are 0, assuming no external ^{1}H spins and that the ground and excited states are well resolved ($\Delta\varpi_{GE} \rightarrow \infty$), it has been derived that[12]

$$R_{ex}(\Delta\omega_E) = \frac{R_{ex}^{\max}\Gamma^2}{\Gamma^2 + \Delta\omega_E^2} \qquad \text{[S18]}$$

with the maximum and half-width at the half maximum of R_{ex}, $R_{ex}^{\max}$ and Γ, given by

$$R_{ex}^{\max} = \frac{k_{ex} p_E \omega_1^2}{\omega_1^2 + k_{ex}(k_{ex} + R_{2,E})} \qquad \text{[S19]}$$

and

$$\Gamma = \sqrt{\frac{k_{ex} + R_{2,E}}{k_{ex}}\omega_1^2 + (k_{ex} + R_{2,E})^2}, \qquad \text{[S20]}$$

respectively, where ω_1 is the weak B_1 field strength in rad/s and $R_{2,E}$ is the transverse relaxation rate of the spin of interest in state E.

Thus, application of a weak B_1 field at $\Delta\omega_E = 0$ leads to a decrease in the intensity of resonance I (major state peak) from 1 (intensity when $\Delta\omega_E \to \infty$) to $\exp(-R_{ex}^{\max} T_{Ex})$, or alternatively, a minor state dip in the CEST profile with size of $1 - \exp(-R_{ex}^{\max} T_{Ex})$ (It is worth noting that this result is identical to that of Eq. [S12] when $\rho_{I,o} = 0$ and $\omega_1 \gg k_{ex}$). The minor state dip line-shape is, in turn, given by $1 - \exp(-R_{ex}(\Delta\omega_E) T_{Ex})$ and in the limit that $R_{ex}^{\max} T_{Ex} \ll 1$ the line-shape is Lorentzian, $R_{ex}(\Delta\omega_E) T_{Ex}$. Several qualitative results can be inferred based on Eqs. [S17]–[S20] and the above discussion, Figure S4: (1) in the regime where $\omega_1 \ll k_{ex}$ increasing B_1 mainly causes an increase of the CEST dip but has little effect on the linewidth, (2) when $\omega_1 \gg k_{ex}$ the CEST peak linewidth increases proportionally to ω_1 while the CEST dip intensity reaches a maximum of $1 - \exp(-k_{ex} p_E T_{Ex})$. Therefore, measurement of multiple CEST profiles with $\omega_1 \gg k_{ex}$ does not add information beyond that from a single CEST profile (see Figure S4A). Extraction of exchange parameters, in general, requires the judicious choice of B_1 values. In general we recommend obtaining a pair of datasets with at least one B_1 value such that $\omega_1 < k_{ex}$ to ensure that exchange parameters can be reliably extracted from global fits (neglecting contributions from external protons that, as discussed above, complicate extraction of exchange parameters from ^{1}H-CEST profiles).

The above discussion focuses on CEST profiles where the dips are singlets as would be obtained in ^{15}N-CEST experiments with ^{1}H decoupling during the CEST element[6], for example. In the case of ^{1}H-CEST where a pair of 'spin-state' selective profiles are recorded and where a difference profile is analyzed the situation is more complex. It is of interest to examine what the optimal B_1 value would be in this case for a given set of exchange parameters. Clearly, for very small fields the CEST dips in each of the spin-state selective profiles would be small, leading to sub-optimal small dips in the difference profile. In contrast, a large B_1 value will optimize the intensity of dips in each of the spin-state selective profiles yet the broad linewidths will lead to subtraction of intensity in the difference profile, a situation that is not ideal either. Optimal B_1 values

can be calculated, however, by noting that the intensities of the excited state CEST dips are given by

$$\begin{aligned} 1-\exp(-R_{ex}(\Delta\omega_E^{\alpha})T_{Ex}), \quad R_{ex}(\Delta\omega_E^{\alpha}) &= \frac{R_{ex}^{\max}\Gamma^2}{\Gamma^2+[\omega_{rf}-(\omega_E-\pi J_{NH})]^2} \\ 1-\exp(-R_{ex}(\Delta\omega_E^{\beta})T_{Ex}), \quad R_{ex}(\Delta\omega_E^{\beta}) &= \frac{R_{ex}^{\max}\Gamma^2}{\Gamma^2+[\omega_{rf}-(\omega_E+\pi J_{NH})]^2} \end{aligned} \qquad \text{[S21]}$$

for the profiles from the $IN^{I\alpha}$ and $IN^{I\beta}$ pathways, respectively, where ω_{rf} is the position of the B_1 field and where ^{1}H and ^{15}N longitudinal relaxation, as well as ^{1}H cross-relaxation, have been neglected. Note that we have assumed that $R_{2,E}$ is the same for the two pathways (*i.e.* transverse cross correlation $\eta_{xy}^{E}=0$ s^{-1}) but this may not be the case. Thus, the line-shape of the dip in the difference profile is

$$L(\omega_{rf})=\exp(-R_{ex}(\Delta\omega_E^{\beta})T_{Ex})-\exp(-R_{ex}(\Delta\omega_E^{\alpha})T_{Ex})\approx[R_{ex}(\Delta\omega_E^{\alpha})-R_{ex}(\Delta\omega_E^{\beta})]T_{Ex}. \qquad \text{[S22]}$$

Maximum values of $L(\omega_{rf})$ are plotted *vs* k_{ex} and B_1 in Figure S5A,B, along with the optimal B_1 that gives a maximum $L(\omega_{rf})$ for a given value of k_{ex}, Figure S5C. Although $L(\omega_{rf})$ will scale with p_E and T_{Ex} the shapes of the profiles will not change in the limit that $R_{ex}^{\max}T_{Ex}\ll 1$. As discussed above, we recommend measurement of p_E and k_{ex} using ^{15}N- or ^{13}C-based CEST methods and choosing the optimal B_1 value that maximizes minor CEST dips in $IN^{I\beta}-IN^{I\alpha}$ difference profiles from the curve of Figure S5C, which is given to excellent approximation by the relation: *optimal* $B_1=5.747k_{ex}^{0.375}$. Figures S5D–I show a number of simulated ^{1}H CEST difference profiles as a function of k_{ex} for $p_E=2\%$. As expected from Figure S5A CEST dips increase initially with k_{ex} (S5D–F) and then decrease as $k_{ex}>\omega_1$ (S5G–I). Notably, even for $k_{ex}=800$ s^{-1} (Figure S5I) minor dips are still observed in the limit that ground and excited states are well separated, suggesting, that small $\Delta\varpi_{GE}$ values are as large an impediment to measuring minor state dips as high k_{ex} rates. Figures S5J–L show that for $R_{2,E}>k_{ex}$, minor state CEST dips decrease as a function of $R_{2,E}$ that is expected from Eq. [S20].

In general, the relatively large $^1J_{HN}$ value (-93 Hz, $\simeq -580$ rad/s) ensures that

CEST peaks can be easily identified in difference CEST profiles for the typical range of k_{ex} values that are usually encountered ($< 500\ s^{-1}$). We have successfully measured ^{1}H $\Delta\varpi_{GE}$ values for L99A T4L at 13.5°C where k_{ex} = 370 s^{-1} (obtained from ^{15}N CEST experiments) using the scheme of Figure 2 (Figure S6). As is the case in all CEST experiments, as k_{ex} becomes larger the linewidths of minor state dips broaden making it more difficult to obtain accurate $\Delta\varpi_{GE}$ values.

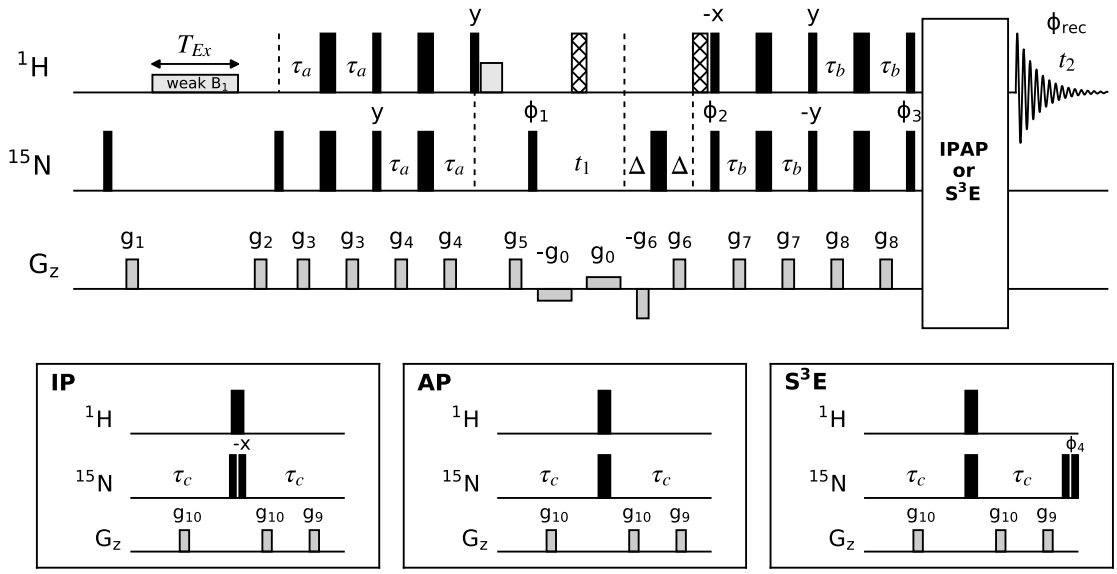

Figure S1. Non-TROSY spin-state selective scheme for the measurement of ^{1}H-CEST profiles in small proteins. Prior to t_1 evolution the pulse scheme is essentially identical to the sequence of Figure 2 with both $IN^{I\alpha}$ and $IN^{I\beta}$ spin-state components of magnetization transferred via ST2 polarization transfer[13] to ^{15}N for chemical shift evolution (t_1). After the t_1 period both pathways are retained, as described previously[14], and these are subsequently separated via IPAP[15,16] or S^{3}E[17] elements at the end of the sequence. Because both pathways are recorded on a per scan basis the signal to noise is improved by $\sqrt{2}$ relative to the case where each pathway is measured independently. Values of the delays are $\tau_a \simeq \tau_b \simeq 1/(4^1J_{HN})$ = 2.70 ms and Δ = 850 μs. All pulses are applied with phase x unless otherwise indicated. The hatched bars denote $90_x180_y90_x$ composite pulses[18]. The following phase cycle is used: $\phi_1 = x, -x$; $\phi_2 = -x$. Quadrature detection in F$_1$ is achieved by inverting the phase of ϕ_2 together with the sign of gradient g$_9$[1]; g$_{10}$ is inverted in concert with g$_9$. Separation of $IN^{I\alpha}$ and $IN^{I\beta}$ pathways can be achieved using either IPAP[15,16] ($\tau_c = 1/(4^1J_{HN})$ = 2.70 ms) or S^{3}E[17] ($\tau_c = 1/(8^1J_{HN})$) schemes, each with similar performance in terms of pathway selection. Note that a value of $\tau_c = 1.39$ ms was found to be optimal for the S^{3}E scheme in terms of isolating each of the two pathways. In the IPAP version $\phi_3 = x$; $\phi_{\rm rec} = x, -x$ for recording in-phase (IP) spectra, while $\phi_3 = -x$; $\phi_{\rm rec} = y, -y$ for recording anti-phase (AP) spectra. In the S^{3}E version a pair of datasets are recorded with $\phi_3 = x$; $\phi_4 = x$; $\phi_{\rm rec} = x, -x$ and with $\phi_3 = -x$; $\phi_4 = -x$; $\phi_{\rm rec} = y, -y$. In both IPAP and S^{3}E approaches the separately recorded datasets are added and subtracted to give CEST spectra corresponding to $IN^{I\alpha}$ and $IN^{I\beta}$ pathways. Gradients g$_1$–g$_9$ are as for the scheme of Figure 2, while the durations (ms) and strengths (in % maximum strength) of the remaining gradients are g$_{10}$: (0.4, 30%), g$_0$ = 0.25%.

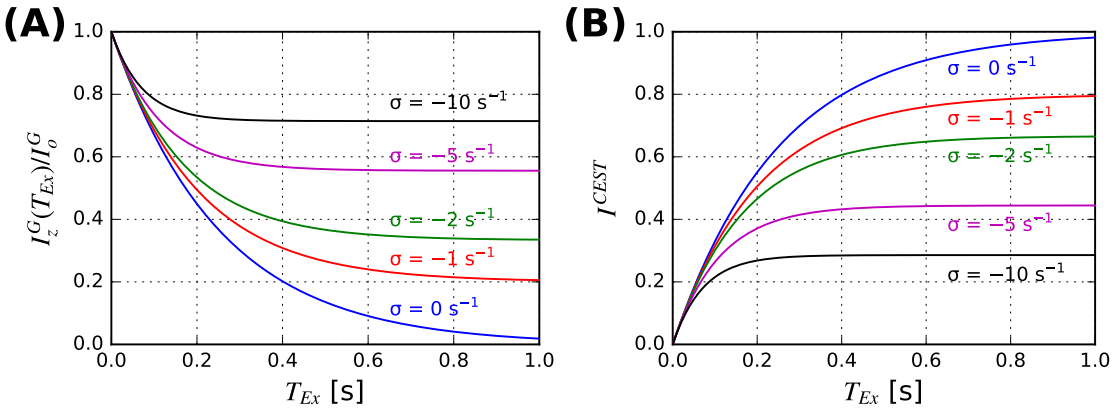

Figure S2. Numerical simulations of the dependence of minor state CEST dip sizes on cross-relaxation rate σ, assuming $p_E = 2\%$, $k_{ex} = 200\ \mathrm{s}^{-1}$, $\Delta\varpi_{GE} \to \infty$, $\omega_1 \gg k_{ex}$, $\rho_{I,o} = \rho_{S,o} = 0\ \mathrm{s}^{-1}$ (Eq. [S11]). (A) The weak B_1 field is placed at ϖ_E and the fractional decrease in the intensity of the ground state peak is plotted *vs* T_{Ex}. (B) Intensity of minor state CEST dip, I^{CEST} *vs* T_{Ex}.

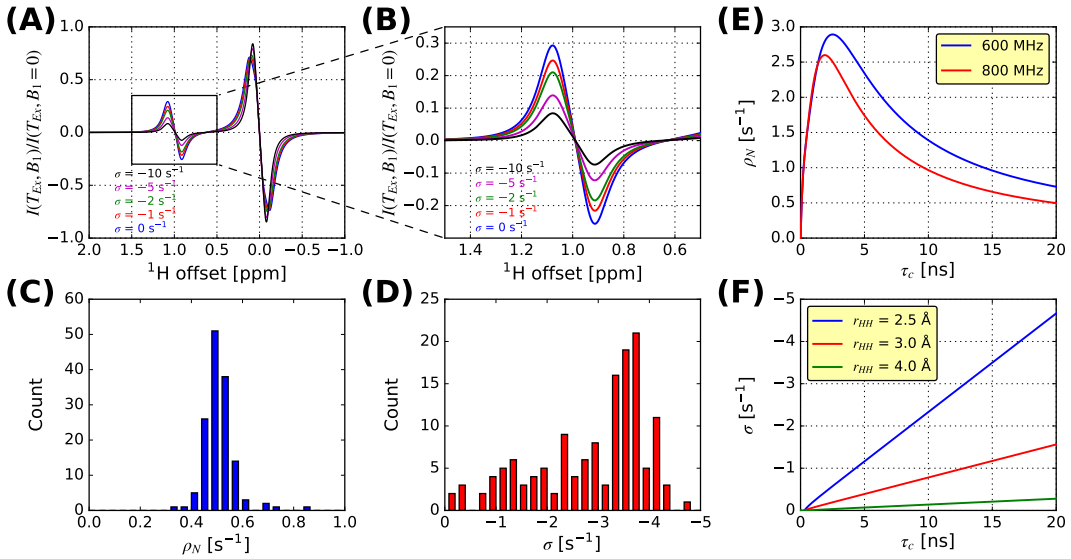

Figure S3. Effects of neighboring ^{1}H spins on intensities of ^{1}H-CEST dips. Simulations were performed using exchange parameters (p_E, k_{ex}) = (2%, 200 s^{-1}), weak CEST B_1 field = 20 Hz, T_{Ex} = 400 ms, ρ_N = 0 s^{-1}, $\rho_{I,o} = \rho_{S,o}$ = 0 s^{-1} (Eq. [S16]), $R_{2,E} = R_{2,G} = 20$ s^{-1}, $\Delta\varpi_{GE}$ = 1.0 ppm with the ground state resonance at 0 ppm, 600 MHz. A pair of dipolar coupled spins I and S were used with spin I exchanging between states G and E. In individual spin-state selective profiles (*i.e.*, before subtraction) baselines are at 1 and major state dips extend from 1 to 0. (A) Comparison of relative sizes of CEST dips for several different cross-relaxation rates between I and S, σ, with the position of the NOE dip at −5 ppm. (B) Expansion of (A) focusing on the minor state CEST dip only. (C,D) Histogram plots of ρ_N and σ for L99A T4L, 9°C, 800 MHz. (E,F) Calculated values of ρ_N and σ *vs* correlation time, τ_c [8]. Values of ρ_N were calculated with the following parameters: $r_{HN} = 1.02$ Å, axially symmetric ^{15}N shift tensor with CSA = −170 ppm [8], square of the amide bond vector order parameter $S^2_{HN} = 1.0$. In (F) different values of σ correspond to different effective amide ^{1}H–^{1}H distances, $r_{HH} = \left\langle \left(\sum_j \left(\frac{1}{r_{ij}^6} \right) \right)^{-\frac{1}{6}} \right\rangle$ where the sum is over all j amide protons in the protein, $i \neq j$, and the angular brackets denote averaging overall all protons i. For reference, the effective distance in perdeuterated L99A T4L is 2.54 Å.

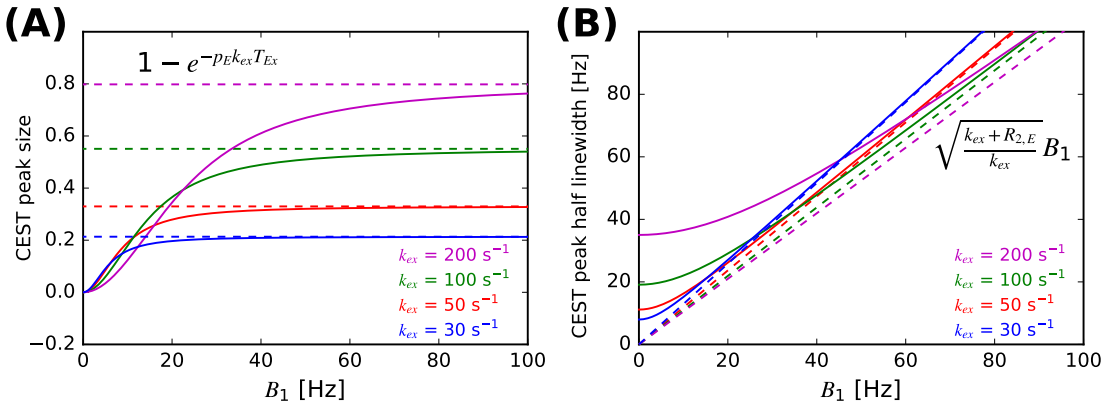

Figure S4. Dependence of minor state CEST peak size (A) and half-linewidth (B) as a function of the weak CEST B_1 field for several different values of k_{ex} (solid lines). The analytical results are based on calculations assuming a singlet CEST dip using Eqs. [S17]–[S20]. All R_1 rates are set to 0 s^{-1}, cross-relaxation is neglected, $R_{2,E} = 20$ s^{-1}, $p_E = 0.02$, T_{Ex} = 400 ms. Major and minor state CEST dips are assumed to be well resolved. The dashed lines in (A) indicate asymptotes of the minor CEST peak sizes expected for the exchange parameters considered $(1 - \exp(-p_E k_{ex} T_{Ex}))$[19] or (B) the asymptote of the minor CEST dip linewidth as $B_1 \gg k_{ex}$, given by $\sqrt{\frac{k_{ex}+R_{2,E}}{k_{ex}}}B_1$.

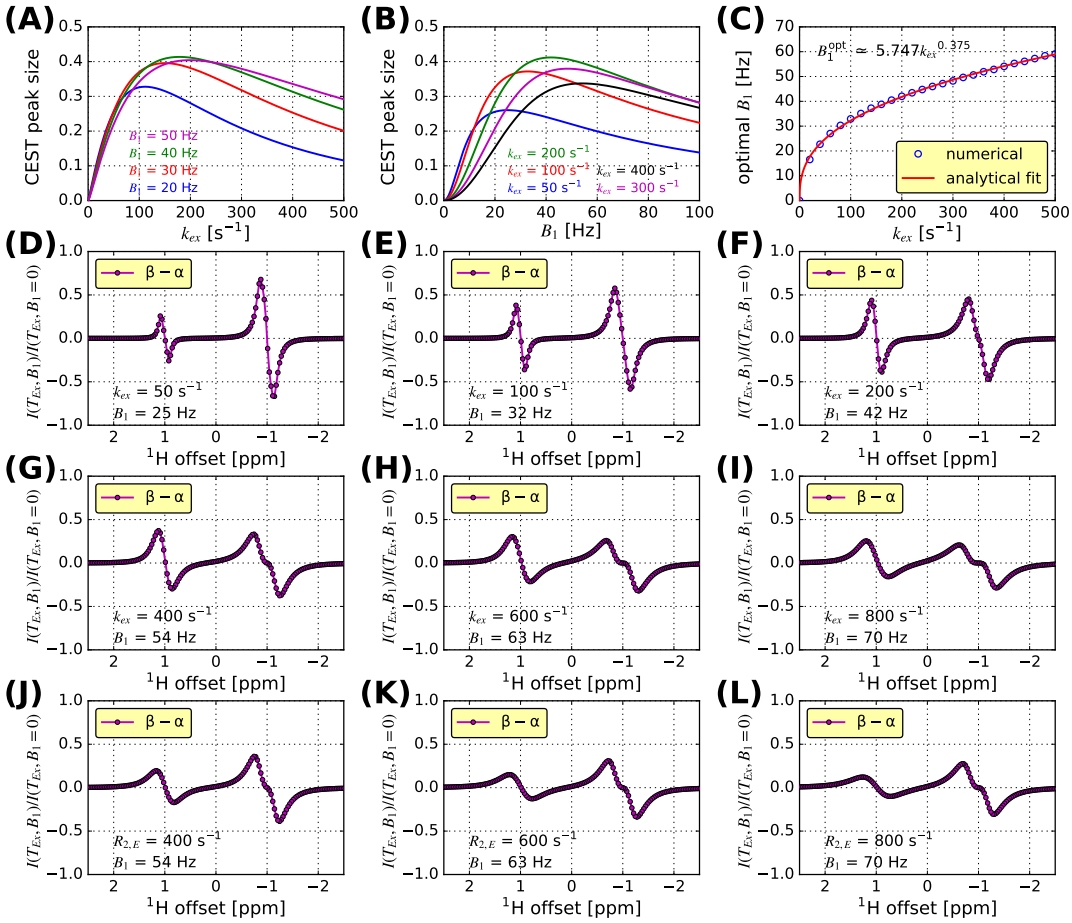

Figure S5. Sensitivity of minor state dips in difference ^{1}H-CEST profiles. Simulations (Eq. [S16]) were performed with $p_E = 2\%$, T_{Ex} = 400 ms, all R_1 rates (both ^{1}H and ^{15}N) are set to 0 s^{-1}, neglecting cross-relaxation, $R_{2,E} = R_{2,G} = 20$ s^{-1}, $\Delta\varpi_{GE}$ = 2.0 ppm, a ground state chemical shift of −1 ppm, 600 MHz. (A) Dependence of CEST peak size on k_{ex} for several CEST fields, B_1. (B) Dependence of CEST peak size on B_1, for several values of k_{ex}. (C) Optimal value of B_1, producing the largest CEST peak size, *vs* k_{ex}; the dependence can be well fitted to a simple functional form $B_1^{opt} = 5.747 k_{ex}^{0.375}$. (D–I) Simulated difference ^{1}H-CEST profiles for a number of k_{ex} rates using optimal B_1 values. (J–L) Simulated difference ^{1}H-CEST profiles *vs* $R_{2,E}$ using B_1 values obtained from (C) with k_{ex} replaced with $R_{2,E}$; the simulation is performed with $k_{ex} = 200$ s^{-1}, $p_E = 2\%$.

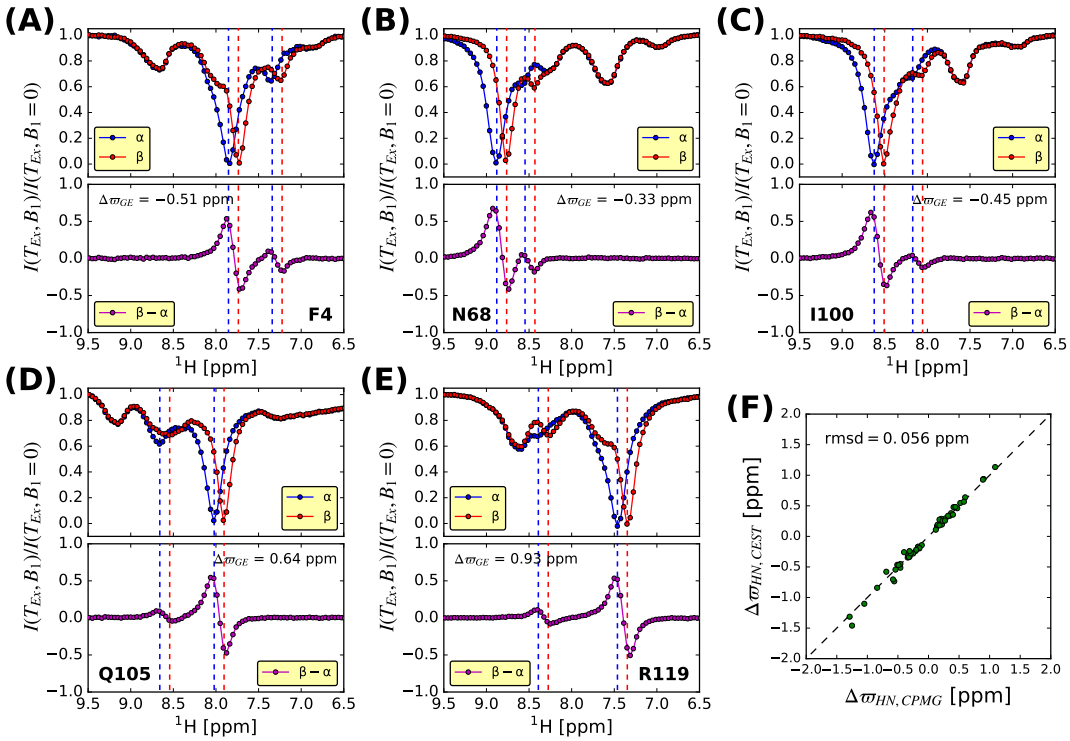

Figure S6. (A–E) Representative ^{1}H-CEST profiles from L99A T4L measured at 13.5°C where $k_{ex} = 370\ s^{-1}$. (F) Linear chemical shift correlation of amide ^{1}H $\Delta\varpi_{GE}$ values from ^{1}H-CPMG (x-axis) and ^{1}H-CEST (y-axis) measurements. ^{1}H CPMG datasets were collected at 25°C[10].

Table S1. Amide ^{1}H chemical shift differences between ground and excited states of the G48A Fyn SH3 domain ($\Delta\varpi_{GE} = \varpi_E - \varpi_G$), as quantified by CEST measurements recorded at 11°C. Amide ^{1}H $\Delta\varpi$ values, assuming that the excited state is a random coil with shifts predicted by the method of Tamiola et al.[20], are also included for comparison ('-' CEST dips cannot be identified from the CEST profile; '*' corresponding residue is either very weak, overlapped or assignment is ambiguous).

Residue	$\Delta\varpi_{H,RC}$ (ppm)	$\Delta\varpi_{GE,CEST}$ (ppm)
Thr 2	-	*
Leu 3	−0.16	-
Phe 4	−0.96	−0.92
Glu 5	−1.34	−1.44
Ala 6	−1.04	−1.06
Leu 7	−1.52	−1.48
Tyr 8	0.96	0.90
Asp 9	−0.39	−0.23
Tyr 10	−0.37	−0.42
Glu 11	0.83	0.87
Ala 12	0.00	−0.20
Arg 13	−1.86	−1.90
Thr 14	−0.70	−0.58
Glu 15	−0.23	-
Asp 16	0.18	-
Asp 17	0.10	-
Leu 18	0.10	0.28
Ser 19	−0.10	-
Phe 20	−0.61	−0.77
His 21	−0.54	−0.61
Lys 22	−0.98	−1.05
Gly 23	−0.67	−0.69
Glu 24	−0.06	-
Lys 25	−0.11	-
Phe 26	−0.98	−1.02
Gln 27	−0.59	−0.61
Ile 28	−1.28	−1.10
Leu 29	−0.59	−0.48
Asn 30	0.64	0.68
Ser 31	−0.47	−0.41

Table S1. *continued*

Residue	$\Delta\varpi_{H,RC}$ (ppm)	$\Delta\varpi_{GE,CEST}$ (ppm)
Ser 32	0.41	0.49
Glu 33	−0.12	−0.24
Gly 34	0.03	−0.16
Asp 35	−0.37	−0.38
Trp 36	0.05	0.25
Trp 37	−2.13	−1.74
Glu 38	−1.11	−0.92
Ala 39	−1.02	−1.21
Arg 40	−0.61	−0.82
Ser 41	−0.44	−0.53
Leu 42	−0.59	−0.60
Thr 43	−0.33	−0.26
Thr 44	0.13	-
Gly 45	0.48	0.40
Glu 46	0.29	0.27
Thr 47	−0.41	−0.23
Ala 48	−0.74	−0.64
Tyr 49	−0.42	*
Ile 50	−1.32	−1.13
Ser 52	0.78	0.74
Asn 53	0.36	0.28
Tyr 54	0.23	0.23
Val 55	0.70	0.58
Ala 56	−0.43	−0.44
Val 58	0.25	0.15
Asp 59	0.02	-
Arg 60	-	0.22

Table S2. Amide ^{1}H chemical shift differences between ground and excited states of L99A T4L ($\Delta\varpi_{GE} = \varpi_E - \varpi_G$), as quantified by CEST measurements at 8.8°C and 13.5°C. Values extracted from CPMG relaxation dispersion experiments at 25°C are also reported for comparison[10] ('-' CEST dips cannot be identified from the CEST profile; '*' corresponding residue is either very weak, overlapped or assignment is ambiguous; '+' CEST dips are likely located outside the scanned region).

Residue	$\Delta\varpi_{GE,CPMG}$, 25°C (ppm)	$\Delta\varpi_{GE,CEST}$, 8.8°C (ppm)	$\Delta\varpi_{GE,CEST}$, 13.5°C (ppm)
Asn 2	±0.04	-	-
Ile 3	0.23	0.26	0.25
Phe 4	−0.46	−0.54	−0.51
Glu 5	−0.09	-	-
Met 6	±0.24	0.30	*
Leu 7	0.14	0.17	0.17
Arg 8	−0.34	−0.33	−0.34
Ile 9	0.08	-	-
Asp 10	±0.00	-	-
Glu 11	−0.16	−0.19	−0.18
Gly 12	-	0.26	0.23
Leu 13	−0.27	−0.29	−0.28
Arg 14	0.28	0.30	0.29
Leu 15	±0.05	-	-
Lys 16	±0.02	-	-
Ile 17	±0.00	-	-
Tyr 18	±0.01	-	-
Lys 19	0.02	-	-
Asp 20	±0.00	-	-
Thr 21	±0.04	-	-
Gly 23	±0.01	-	-
Tyr 24	0.06	-	-
Tyr 25	±0.00	-	-
Thr 26	0.07	-	-
Ile 27	0.08	-	-
Gly 28	0.11	-	-
Ile 29	0.72	+	+
Gly 30	0.21	0.23	0.23
His 31	−0.11	-	-
Leu 32	−0.21	−0.25	−0.24

Table S2. *continued*

Residue	$\Delta\varpi_{GE,CPMG}$, 25°C (ppm)	$\Delta\varpi_{GE,CEST}$, 8.8°C (ppm)	$\Delta\varpi_{GE,CEST}$, 13.5°C (ppm)
Leu 33	−0.05	-	-
Thr 34	±0.01	-	-
Lys 35	±0.00	-	-
Ser 36	±0.05	-	-
Ser 38	±0.00	-	-
Leu 39	±0.00	-	-
Asn 40	±0.00	-	-
Ala 41	±0.00	-	-
Ala 42	±0.01	-	-
Lys 43	±0.00	-	-
Ser 44	±0.00	-	-
Leu 46	±0.00	-	-
Asp 47	±0.09	-	-
Lys 48	±0.04	-	-
Ala 49	±0.00	-	-
Ile 50	±0.06	-	-
Gly 51	±0.07	-	-
Arg 52	0.01	-	-
Asn 53	±0.00	-	-
Thr 54	±0.01	-	-
Asn 55	±0.00	-	-
Gly 56	±0.00	-	-
Val 57	±0.01	-	-
Ile 58	−0.06	-	-
Thr 59	±0.00	-	-
Lys 60	±0.00	-	-
Asp 61	±0.00	-	-
Glu 62	±0.05	-	-
Ala 63	±0.00	-	-
Glu 64	±0.00	-	-
Lys 65	0.23	0.24	0.24
Leu 66	±0.04	-	-
Phe 67	−0.17	−0.18	−0.17
Asn 68	−0.31	−0.34	−0.33
Gln 69	0.19	0.19	0.19
Asp 70	0.52	0.56	0.55
Val 71	−0.17	−0.17	−0.17

Table S2. *continued*

Residue	$\Delta\varpi_{GE,CPMG}$, 25°C (ppm)	$\Delta\varpi_{GE,CEST}$, 8.8°C (ppm)	$\Delta\varpi_{GE,CEST}$, 13.5°C (ppm)
Asp 72	−0.15	−0.20	−0.20
Ala 73	0.37	0.38	0.38
Ala 74	−0.33	−0.32	−0.32
Val 75	−0.56	−0.78	−0.73
Arg 76	0.35	0.33	0.34
Gly 77	0.21	0.29	0.29
Ile 78	−0.51	−0.46	−0.46
Leu 79	−0.05	-	-
Arg 80	0.32	0.34	0.34
Asn 81	−0.12	-	-
Ala 82	−0.11	−0.14	−0.14
Lys 83	−0.04	-	-
Leu 84	−0.25	−0.29	−0.28
Lys 85	−0.33	−0.28	−0.30
Val 87	0.06	-	-
Tyr 88	−0.06	-	-
Asp 89	±0.02	-	-
Ser 90	0.08	-	-
Leu 91	0.20	0.21	0.21
Asp 92	±0.03	-	-
Ala 93	−0.03	-	-
Val 94	0.12	0.11	0.11
Arg 95	0.15	0.16	0.19
Arg 96	−0.08	-	-
Ala 97	−0.15	−0.19	−0.19
Ala 98	0.23	-	-
Ala 99	0.16	-	-
Ile 100	−0.46	−0.47	−0.45
Asn 101	−0.32	−0.34	−0.34
Met 102	0.08	-	-
Val 103	−0.84	−0.83	−0.84
Phe 104	−1.29	−1.32	−1.31
Gln 105	0.60	0.67	0.64
Met 106	0.20	-	-
Gly 107	−0.64	−0.69	*
Glu 108	−0.29	−0.27	−0.28
Thr 109	0.22	0.28	*

Table S2. *continued*

Residue	$\Delta\varpi_{GE,CPMG}$, 25°C (ppm)	$\Delta\varpi_{GE,CEST}$, 8.8°C (ppm)	$\Delta\varpi_{GE,CEST}$, 13.5°C (ppm)
Gly 110	1.09	1.17	1.13
Val 111	0.41	0.49	0.48
Ala 112	0.22	0.14	0.19
Gly 113	0.90	0.96	0.94
Phe 114	0.18	0.17	0.18
Thr 115	0.58	0.58	0.57
Asn 116	−0.69	−0.59	−0.58
Ser 117	−1.05	−1.17	−1.10
Leu 118	−1.25	−1.52	−1.46
Arg 119	0.89	0.96	0.93
Met 120	−0.20	−0.21	−0.22
Leu 121	−0.49	−0.47	−0.47
Gln 122	0.47	0.46	0.46
Gln 123	±0.07	-	-
Lys 124	−0.10	-	-
Arg 125	±0.04	-	-
Trp 126	0.13	-	-
Asp 127	±0.02	-	-
Glu 128	±0.07	-	-
Ala 129	−0.02	-	-
Ala 130	0.11	-	-
Val 131	0.09	-	-
Asn 132	±0.14	-	-
Leu 133	−0.10	-	-
Ala 134	0.40	0.36	0.36
Lys 135	0.11	-	-
Ser 136	±0.03	-	-
Arg 137	−0.40	−0.26	−0.26
Trp 138	0.18	0.27	0.27
Tyr 139	0.23	0.26	0.25
Asn 140	-	-	-
Gln 141	−0.54	−0.57	−0.54
Thr 142	−0.58	−0.74	−0.70
Asn 144	0.21	-	-
Arg 145	0.07	-	-
Ala 146	0.44	0.49	0.48
Lys 147	−0.23	-	-

Table S2. *continued*

Residue	$\Delta\varpi_{GE,CPMG}$, 25°C (ppm)	$\Delta\varpi_{GE,CEST}$, 8.8°C (ppm)	$\Delta\varpi_{GE,CEST}$, 13.5°C (ppm)
Arg 148	0.20	*	*
Val 149	0.27	0.26	0.26
Ile 150	−0.27	-	-
Thr 151	−0.18	-	-
Thr 152	0.08	-	-
Phe 153	0.12	-	-
Arg 154	−0.31	−0.22	−0.24
Thr 155	0.07	-	-
Gly 156	±0.00	-	-
Thr 157	±0.04	-	-
Trp 158	−0.09	-	-
Asp 159	±0.02	-	-
Ala 160	±0.06	-	-
Tyr 161	±0.00	-	-
Lys 162	0.09	-	-
Asn 163	0.01	-	-
Leu 164	0.08	-	-

References

[1] L. E. Kay, P. Keifer, T. Saarinen, *J. Am. Chem. Soc.* **1992**, *114*, 10663–10665.

[2] F. A. A. Mulder, R. Otten, R. M. Scheek, *J. Biomol. NMR* **2011**, *51*, 199–207.

[3] M. Guenneugues, P. Berthault, H. Desvaux, *J. Magn. Reson.* **1999**, *136*, 118–126.

[4] G. Bouvignies, P. Vallurupalli, L. E. Kay, *J. Mol. Biol.* **2014**, *426*, 763–774.

[5] G. Bouvignies, P. Vallurupalli, D. F. Hansen, B. E. Correia, O. Lange, A. Bah, R. M. Vernon, F. W. Dahlquist, D. Baker, L. E. Kay, *Nature* **2011**, *477*, 111–114.

[6] P. Vallurupalli, G. Bouvignies, L. E. Kay, *J. Am. Chem. Soc.* **2012**, *134*, 8148–8161.

[7] F. Delaglio, S. Grzesiek, G. W. Vuister, G. Zhu, J. Pfeifer, A. Bax, *J. Biomol. NMR* **1995**, *6*, 277–293.

[8] J. Cavanagh, W. J. Fairbrother, A. G. Palmer, M. Rance, N. Skelton, *Protein NMR Spectroscopy*, Elsevier Academic Press, London, 2nd ed., **2007**.

[9] H. M. McConnell, *J. Chem. Phys.* **1958**, *28*, 430–431.

[10] G. Bouvignies, L. E. Kay, *J. Phys. Chem. B* **2012**, *116*, 14311–14317.

[11] P. Allard, M. Helgstrand, T. Hard, *J. Magn. Reson.* **1998**, *134*, 7–16.

[12] M. Zaiss, P. Bachert, *NMR Biomed.* **2013**, *26*, 507–518.

[13] K. V. Pervushin, G. Wider, K. Wuthrich, *J. Biomol. NMR* **1998**, *12*, 345–348.

[14] D. W. Yang, L. E. Kay, *J. Biomol. NMR* **1999**, *13*, 3–10.

[15] M. Ottiger, F. Delaglio, A. Bax, *J. Magn. Reson* **1998**, *131*, 373–378.

[16] D. W. Yang, K. Nagayama, *J. Magn. Reson.* **1996**, *118*, 117–121.

[17] I. C. Felli, R. Pierattelli, *Prog. Nucl. Magn. Reson. Spectrosc.* **2015**, *84*, 1–13.

[18] M. H. Levitt, R. Freeman, *J. Magn. Reson.* **1979**, *33*, 473–476.

[19] T. Yuwen, A. Sekhar, L. E. Kay, *J. Biomol. NMR* **2016**, *65*, 143–156.

[20] K. Tamiola, B. Acar, F. A. A. Mulder, *J. Am. Chem. Soc.* **2010**, *132*, 18000–18003.

```
/* 1H_CEST_Iz_TRsss_lek_800_cpz

  This pulse sequence will allow one to perform the following experiment:
  1H CEST when magnetization is of the form Iz with 15N-1H HSQC readout.
  Takes the difference between 1H Z magnetization up and down

  TROSY spin state selective transfer:
    l3=0: I(TR) ---> N(TR) ---> I(TR)
    l3=1: I(AT) ---> N(TR) ---> I(TR)

  Pervusion TROSY based hsqc including a flag for gradient coherence transfer select
ion

  Note: Identical trosy selection can be achieved by inverting the phase of the firs
t 1H 90 after t1
        along with the final 15N 90 and then inverting the first 2 or last 2 receive
r phases
        Addition of coherence transfer gradients does not change the cycle

  If gd_sel is used then the min phase cycle is 2
  If gd_sel is not used then the min phase cycle is 4

  To callibrate B1 field: set -Dcal_HB1
    - calibrate by setting 1H decoupling field to 0
    - sit on one of the 1H multiplet components and evolution will be of the other c
omponent
    - calibration is done with magnetization Iz at the very beginning

  Used with N15cest_make_fq_list.c (ccode) which makes the frequency list
  Used with N15cest_cal_B1.c (ccode)
  Used with move_lek_cest_fq which moves the freq list to f1
  Used with move_lek_cest_B1 which moves the list of times to vd list

  Hsteady_flg is for measuring the decay of Hz magnetization to extract R1 rates

  Written from 1H_CEST_Iz_trosy_lek_600_cp on Sept 26(!) 2016 by LEK

*/

prosol relations=<triple>

#include <Avance.incl>
#include <Grad.incl>
#include <Delay.incl>

/***********************/
/*   Define phases     */
/***********************/
#define zero ph=0.0
#define one ph=90.0
#define two ph=180.0
#define three ph=270.0

/*************************/
/*    Define delays      */
/*************************/
define delay hscuba      /* length of 1/2 scuba delay */
  "hscuba=30m"
define delay taua        /* 1 / 4J(XH)                */
  "taua=d3"              /* 1s/(4*105) use JNH=105 to decrease the tauxh duration */
define delay taub        /* 1 / 4J(XH)                */
  "taub=d5"              /* 1s/(4*95) use JNH=95 for tauxh duration */
define delay BigT1
  "BigT1=d14"
define delay BigT
  "BigT=d15"

#if !defined(cal_HB1) && !defined(cal_HR1)
  define delay time_T1
    "time_T1=d17"        /* CEST duration - typically 100-500 ms */
#endif

"d11=30m"
```

```
"in0=inf1/2"              /* t1/2 increment */

/*****************************************************************/
/* f1180: Start t1 at half dwell to get -90/180 phase correction */
/*        in F1 (15N) dim - set zgoptns -Df1180                  */
/*****************************************************************/
#ifdef f1180
  "d0=(in0)/2"
#else
  "d0=0.1u"
#endif

/************************/
/*    Define pulses     */
/************************/
define pulse dly_pg1      /* Messrle purge pulse */
  "dly_pg1=5m"
define pulse dly_pg2      /* Messrle purge pulse */
  "dly_pg2=dly_pg1/1.62"
define pulse pwh
  "pwh=p1"                /* 1H hard pulse at power level pl1 (tpwr) */
define pulse pw_sl
  "pw_sl=p13"             /* 1H water selective pulse at power level pl13 (tpwrsl) */

#if defined(Hsteady_flg) || !defined(gd_sel)
  define pulse pw_sl1
    "pw_sl1=p14"          /* 1H water selective pulse at power level pl14 (tpwrsl1) *
/
#endif

define pulse pwn
  "pwn=p3"                /* PW90 for N pulse at power level pl3 (dhpwr2)  */

#ifdef c_flg
  define pulse pwc_ad     /* 13C adiabatic pulse at power level spw22(pwc_ad) */
    "pwc_ad=p22"
#endif

#ifdef N_sel
  define pulse pwn_sl
    "pwn_sl=p32"
#endif

/*********************************/
/*    Define other parameters    */
/*********************************/
define loopcounter Nphase
  "Nphase=1"

#ifdef cal_HB1
  define list<delay> time_cal=<t1list_calB1>
#else
#ifdef cal_HR1
  define list<delay> time_cal=<t1list_calR1>
#else
  define list<frequency> H_offset=<$FQ1LIST>
#endif
#endif

/*****************************************************/
/* Assign cnsts to check validity of parameter range */
/*****************************************************/
#ifdef fsat
  "cnst10=plw10"          /* tsatpwr - set max at 0.00005W */
#endif

#ifdef mess_flg
  "cnst11=plw11"          /* tpwrmess pl11 - set max at 2.0W */
#endif

  "cnst13=spw13"          /* tpwrsl - set max at 0.001W" */

#if defined(Hsteady_flg) || !defined(gd_sel)
```

```
  "cnst14=spw14"          /* tpwrsl1 - set max at 0.001W" */
#endif

#ifdef c_flg
  "cnst22=spw22"          /* d_ad - set max at 57W */
#endif

#ifdef N_sel
  "cnst32=spw32"          /* power level for 15N selective pulse */
#endif

/*************************************************/
/* Set the weak H-amide B1 field for irradiation */
/*************************************************/
"p15=1000000.0/(4.0*cnst16)"
"plw15=plw1*(pwh)*(pwh)/((p15)*(p15))"
"cnst15=plw15"

/*****************************************************/
/* Set phase alignment and offset for shaped pulses  */
/*****************************************************/
"spoal13=0"
"spoal14=0"
"spoff13=0"
"spoff14=0"

/****************************/
/* Initialize loop counters */
/****************************/
"l2=0"
"l3=0"

"acqt0=0"
baseopt_echo

1 ze
/*****************************************/
/*   Check Validity of Parameter Range   */
/*****************************************/
#ifdef fsat
  if "cnst10 > 0.00005"
  {
    2u
    print "error: tsatpwr pl10 too large !!!  "
    goto HaltAcqu
  }
#endif

#ifdef mess_flg
  if "cnst11 > 2.0"
  {
    2u
    print "error:tpwrmess pl11 too large !!!  "
    goto HaltAcqu
  }
#endif

  if "cnst13 > 0.002"
  {
    2u
    print "error: tpwrsl spw13 too large !!!  "
    goto HaltAcqu
  }

#if defined(Hsteady_flg) || !defined(gd_sel)
  if "cnst14 > 0.002"
  {
    2u
    print "error: tpwrsl1 spw14 too large !!!  "
    goto HaltAcqu
  }
#endif
```

```
  if "cnst15 > 0.01"
  {
    2u
    print "error: cnst15 - power in W for 1H CEST is too large !!!  "
    goto HaltAcqu
  }

  if "cnst16 > 250"
  {
    2u
    print "error: cnst16 - weak 1H B1 field strength in Hz must be <= 250 Hz !!!  "
    goto HaltAcqu
  }

#ifdef c_flg
  if "cnst22 > 50"
  {
    2u
    print "error: pwc_ad spw22 is too large !!!  "
    goto HaltAcqu
  }
#endif

#ifdef N_sel
  if "cnst32 > 35"
  {
    2u
    print "error: spw23 is too large < 55W !!!  "
    goto HaltAcqu
  }
#endif

#if !defined(cal_HB1) && !defined(cal_HR1)
  if "time_T1 > 0.5s"
  {
    2u
    print "error: time_T1 is too long"
    goto HaltAcqu
  }
#endif

2 d11
/*****************************************/
/* Continue to check real time variables */
/*****************************************/
#ifdef cal_HB1
  "DELTA=time_cal[l2]"
  if "DELTA > 500m"
  {
    2u
    print "error: time_cal (evolution time during B1 calib is too long < 500 m"
    goto  HaltAcqu
  }
#endif

/*************************************************/
/*   Presaturation Period                        */
/*   option for Messrlie purge zgoptn -Dmess_flg  */
/*************************************************/
#ifdef mess_flg
  20u pl11:f1
  (dly_pg1 ph26):f1
  20u
  (dly_pg2 ph27):f1
  20u pl10:f1
#endif /*mess_flg*/

#ifdef fsat
  4u pl10:f1
  d1 cw:f1 ph26
  4u do:f1
  2u pl1:f1
#ifdef fscuba
```

```
  hscuba
  (pwh ph26):f1
  (pwh*2 ph27):f1
  (pwh ph26):f1
  hscuba
#endif /*fscuba*/
#else
  2u pl1:f1
  d1
#endif /*fsat*/

  20u UNBLKGRAD

/*****************************************/
/* Erase 15N equilibrium magnetization */
/*****************************************/
  2u pl3:f3
  (pwn ph26):f3

  2u
  p51:gp1
  d16

/*************************************************/
/*  +/- phase cycle on 1H prior to CEST period    */
/*************************************************/
#ifdef Hsteady_flg
  2u
  (pw_sl1:sp14 ph27):f1
  2u pl1:f1
  (pwh ph26 pwh*2 ph21 pwh ph26):f1
  (pw_sl:sp13 ph22):f1
  2u

  2u
  p51:gp1
  d16
#endif /*Hsteady_flg*/

/*****************************************/
/*   CEST portion on Hz magnetization   */
/*****************************************/
  2u pl15:f1
#ifdef cal_HB1
  "DELTA=time_cal[l2]"
  2u fq=cnst1:f1
  DELTA cw:f1 ph26
  2u do:f1
#else
#ifdef cal_HR1
  "DELTA=time_cal[l2]"
  DELTA
#else
  2u fq=H_offset:f1
  time_T1 cw:f1 ph26
  2u do:f1
#endif /*cal_HR1*/
#endif /*cal_HB1*/
  20u fq=0:f1 pl1:f1

  2u
  p52:gp2
  d16

/*******************************************/
/*   TROSY-type H-N transfer:              */
/*   l3=0: Hx(TR) ---> Nx(TR) ---> Hx(TR)  */
/*   l3=1: Hx(AT) ---> Nx(TR) ---> Hx(TR)  */
/*******************************************/
  if "l3%2 == 0" {
    (pwn ph26):f3
  }
  else {
```

```
    (pwn ph28):f3
  }

  2u
  p53:gp3
  d16

  "DELTA = taua - 2u - p53 - d16"
  DELTA

  (center (pwh*2 ph26):f1 (pwn*2 ph26):f3)

  DELTA

  2u
  p53:gp3
  d16

  (pwn ph27):f3
  (pwh ph26):f1

  2u
  p54:gp4
  d16

#ifdef N_sel
  "DELTA = taua - 2u - p54 - d16 - pwn_sl*0.5"
#else
  "DELTA = taua - 2u - p54 - d16"
#endif
  DELTA

#ifdef N_sel
  (center (pwh*2 ph26):f1 (pwn_sl:sp32 ph26):f3)
#else
  (center (pwh*2 ph26):f1 (pwn*2 ph26):f3)
#endif

  DELTA

  2u
  p54:gp4
  d16

  (pwh ph27):f1

  /* shaped pulse */
  4u
  (pw_sl:sp13 ph28):f1
  2u pl1:f1
  /* end shaped pulse */

  2u pl3:f3
  p55:gp5
  d16

/**********************/
/*   15N labeling     */
/**********************/
#ifndef Hsteady_flg
  if "Nphase %2 == 1" {
    (pwn ph1):f3
  }
  else {
    (pwn ph2):f3
  }
#else
  if "Nphase %2 == 1" {
    (pwn ph11):f3
  }
  else {
    (pwn ph12):f3
  }
```

```
#endif /*Hsteady_flg*/

#ifdef c_flg
  if "d0 - pwc_ad*0.5 > 2u"
  {
    "DELTA = d0 - pwc_ad*0.5"
    DELTA
    (pwc_ad:sp22 ph26):f2
    DELTA
  }
  else
  {
    d0
    d0
  }
#else
  d0
  d0
#endif /*c_flg*/

#ifdef gd_sel
  2u
  p56:gp6*-1.0
  d16

  "DELTA = BigT - 2u - p56 - d16"
  DELTA

  (pwn*2 ph26):f3

  2u
  p56:gp6*1.0
  d16

  "DELTA = BigT - 2u - p56 - d16 + pwn*4.0/PI"
  DELTA
#endif /*gd_sel*/

/*************************************/
/*   TROSY-type N->H back transfer   */
/*************************************/
  (pwh ph3):f1

  /* shaped pulse */
  4u
  (pw_sl:sp13 ph4):f1
  2u pl1:f1
  /* end shaped pulse */

  2u
  p57:gp7
  d16

  "DELTA = taub - 4u - pw_sl - 2u - 2u - p57 - d16"
  DELTA

  (center (pwh*2 ph26):f1 (pwn*2 ph5):f3)

  DELTA

  2u
  p57:gp7
  d16

  /* shaped pulse */
  4u
  (pw_sl:sp13 ph26):f1
  2u pl1:f1
  /* end shaped pulse */

  (pwh ph26):f1
  (pwn ph6):f3
```

```
  2u
  p58:gp8
  d16

#ifdef gd_sel
  "DELTA = taub - 2u - p58 - d16"
  DELTA
#else
  "DELTA = taub - 2u - p58 - d16 - 4u - pw_sl1 - 2u"
  DELTA

  /* shaped pulse */
  4u
  (pw_sl1:sp14 ph7:r):f1
  2u pl1:f1
  /* end shaped pulse */
#endif /*gd_sel*/

  (center (pwh*2 ph26):f1 (pwn*2 ph26):f3)

#ifdef gd_sel
  "DELTA = taub - 2u - p58 - d16"
#else
  /* shaped pulse */
  4u
  (pw_sl:sp13 ph8:r):f1
  2u pl1:f1
  /* end shaped pulse */

  "DELTA = taub - 4u - pw_sl - 2u - 2u - p58 - d16 + pwh*2.0/PI - 4u - de"
#endif /*gd_sel*/

  DELTA

  2u
  p58:gp8
  d16

#ifdef gd_sel
  (pwn ph28):f3

  BigT1

  (pwh*2 ph26):f1

  "DELTA = BigT1 - 2u - p59 - d16 - pwh*2.0/PI - 4u - de"
  DELTA

  2u
  p59:gp9*EA
  d16

  4u BLKGRAD
#else
  4u BLKGRAD
  (pwn ph28):f3
#endif /*gd_sel*/

/*************************************/
/*   Test how much water left        */
/*   set d13=AQ and zgoptn -Dwater   */
/*   also use small value of rg      */
/*************************************/
#ifdef water
  if "nsdone == 0"
  {
    d13
    d1
    (pwh*0.1 ph26):f1
  }
  else
  {
    d13
```

```
  }
#endif

/*************************************/
/*   Signal detection and looping    */
/*************************************/
  go=2 ph31
  d11 mc #0 to 2

  F3QF(calclc(l3,1))
#if defined(cal_HB1) || defined(cal_HR1)
  F2QF(calclc(l2,1))
#else
  F2QF(calclist(H_offset,1))
#endif /*cal_HB1, cal_HR1*/
  F1EA(calgrad(EA) & calph(ph3, +180) & calph(ph4, +180) & calph(ph6, +180) & calph(
ph31, +180) & calclc(Nphase, 1), caldel(d0, +in0) & calph(ph1, +180) & calph(ph2, +1
80) & calph(ph11, +180) & calph(ph12, +180) & calph(ph31, +180))

HaltAcqu, 1m
exit

ph1=1 3 2 0
ph2=1 3 0 2
ph3=1
ph4=3
ph5=0 0 0 0 1 1 1 1 2 2 2 2 3 3 3 3
ph6=3
ph7=2
ph8=2
ph11=1 1 2 2
ph12=1 1 0 0
ph21=2 1
ph22=3 1
ph26=0
ph27=1
ph28=2
ph29=3
ph31=3 1 2 0 1 3 0 2

;d1 : Repetition delay d1
;d3 : taua ~1/4J(NH) 2.70 ms
;d5 : taub ~1/4J(NH) 2.70 ms
;d11 : disk read/write delay
;d14 : BigT1 set to 500 us
;d15 : BigT set to 850 us
;d16 : gradient recovery delay 200 us
;d17 : time_T1, time for CEST, typically several 100s of ms
;pl1 : tpwr - power level for 1H pulses
;pl3 : dhpwr2 -  power level for N hard pulses
;pl10 : tsatpwr - power level for water presat
;pl11 : tpwrmess - power level for Messerle purge
;spw13 : tpwrsl - power level for water selective pulse pw_sl
;spw14 : tpwrsl1 - power level for water selective pulse pw_sl1
;p1 : pwh - 1H 90 degree pulse
;p3 : pwn - 15N 90 degree pulse
;p13 : pw_sl
;p14 : pw_sl1
;p22 : pwc_ad -  adiabatic C180 pulse width
;p32 : pwn_sl for selective pulse on amide N15s
;p51 : gradient pulse 51                                  [400 usec]
;p52 : gradient pulse 52                                  [1000 usec]
;p53 : gradient pulse 53                                  [500 usec]
;p54 : gradient pulse 54                                  [256 usec]
;p55 : gradient pulse 55                                  [1500 usec]
;p56 : gradient pulse 56                                  [625 usec]
;p57 : gradient pulse 57                                  [256 usec]
;p58 : gradient pulse 58                                  [256 usec]
;p59 : gradient pulse 59                                  [256 usec]
;spnam13 : shape for pw_sl
;spnam14 : shape for pw_sl1
;spnam22 : shape for pwc_ad
;spnam32 : shape for pwn_sl
```

```
;phcor7 : phase correction for ph7 of pw_sl1
;phcor8 : phase correction for ph8 of pw_sl
;cnst1 : offset (Hz) for B1 calibration from o1
;cnst16 : weak CEST 1H B1 field in Hz
;l2 : pointer to delay value for calibration of B1
;l3 : pointer to switch between two TROSY transfer pathways
;inf1 : 1/SW(X) = 2*DW(X)
;in0 : 1/(2*SW(x))=DW(X)
;nd0 : 2
;ns : 2*n
;FnMODE : echo-antiecho

;use gradient ratio:    gp 6 : gp 9
;                         80 : -39.5

;for z-only gradients:
;gpz1: -25%
;gpz2: 15%
;gpz3: -50%
;gpz4: 23%
;gpz5: -70%
;gpz6: 80%
;gpz7: 60%
;gpz8: 15%
;gpz9: -39.5%

;use gradient files:
;gpnam1: SMSQ10.32
;gpnam2: SMSQ10.32
;gpnam3: SMSQ10.32
;gpnam4: SMSQ10.32
;gpnam5: SMSQ10.32
;gpnam6: SMSQ10.32
;gpnam7: SMSQ10.32
;gpnam8: SMSQ10.32
;gpnam9: SMSQ10.32

;zgoptns: Dfsat, Dfscuba, Dmess_flg, Df1180, Dgd_sel, Dc_flg, DN_sel, Dcal_HB1, DHst
eady_flg, Dcal_HR1
```

```
/* 1H_CEST_Iz_noTRsss_lek_800_cpz

  Used for measurement of amide 1H CEST in small proteins so dont use TROSY

  This pulse sequence will allow one to perform the following experiment:
  1H CEST when magnetization is of the form Iz with 15N-1H HSQC readout.
  Takes the difference between 1H Z magnetization up and down

  Spin state selective transfer:
    l3=0: I(TR/AT) ---> N(TR/AT) ---> I(TR/AT) ---> IP
    l3=1: I(TR/AT) ---> N(TR/AT) ---> I(TR/AT) ---> AP

  To callibrate B1 field: set -Dcal_HB1

  Min phase cycle is 2

  Used with N15cest_make_fq_list.c (ccode) which makes the frequency list
  Used with N15cest_cal_B1.c (ccode)
  Used with move_lek_cest_fq which moves the freq list to f1
  Used with move_lek_cest_B1 which moves the list of times to vd list

  s3_flg is used for the alternative shorter version of IPAP scheme

  Hsteady_flg is for measuring the decay of Hz magnetization to extract R1 rates

  Written by LEK and TY on Oct 2, 2016

*/

prosol relations=<triple>

#include <Avance.incl>
#include <Grad.incl>
#include <Delay.incl>

/***********************/
/*   Define phases     */
/***********************/
#define zero ph=0.0
#define one ph=90.0
#define two ph=180.0
#define three ph=270.0

/*************************/
/*    Define delays      */
/*************************/
define delay hscuba      /* length of 1/2 scuba delay */
  "hscuba=30m"
define delay taua        /* 1 / 4J(XH)                */
  "taua=d3"              /* 1s/(4*105) use JNH=105 to decreas the tauxh duration */
define delay taub        /* 1 / 4J(XH)                */
  "taub=d5"              /* 1s/(4*95) use JNH=95 for tauxh duration */

define delay tauc        /* 1 / 4J(XH) or 1 / 8J(XH)  */
#ifndef s3_flg
  "tauc=2.7m"
#else
#ifndef cal_HB1
  "tauc=1.39m"
#else
  "tauc=5.4m"
#endif /*cal_HB1*/
#endif /*s3_flg*/

define delay BigT
  "BigT=d15"

#if !defined(cal_HB1) && !defined(cal_HR1)
  define delay time_T1
    "time_T1=d17"        /* CEST duration - typically 100-500 ms */
#endif

"d11=30m"
```

```
"in0=inf1/2"              /* t1/2 increment */

/*****************************************************************/
/* f1180: Start t1 at half dwell to get -90/180 phase correction */
/*        in F1 (15N) dim - set zgoptns -Df1180                  */
/*****************************************************************/
#ifdef f1180
  "d0=(in0)/2"
#else
  "d0=0.1u"
#endif

/*************************/
/*    Define pulses      */
/*************************/
define pulse dly_pg1      /* Messrle purge pulse */
  "dly_pg1=5m"
define pulse dly_pg2      /* Messrle purge pulse */
  "dly_pg2=dly_pg1/1.62"
define pulse pwh
  "pwh=p1"                /* 1H hard pulse at power level pl1 (tpwr) */

#ifdef Hsteady_flg
  define pulse pw_sl
    "pw_sl=p13"           /* 1H water selective pulse at power level pl13 (tpwrsl) */
#endif

define pulse pw_sl1
  "pw_sl1=p14"            /* 1H water selective pulse at power level pl14 (tpwrsl1) *
/

define pulse pwn
  "pwn=p3"                /* PW90 for N pulse at power level pl3 (dhpwr2)  */

#ifdef c_flg
  define pulse pwc_ad     /* 13C adiabatic pulse at power level spw22(d_ad) */
    "pwc_ad=p22"
#endif

#ifdef N_sel
  define pulse pwn_sl
    "pwn_sl=p32"
#endif

/*********************************/
/*    Define other parameters    */
/*********************************/
#ifdef cal_HB1
  define list<delay> time_cal=<t1list_calB1>
#else
#ifdef cal_HR1
  define list<delay> time_cal=<t1list_calR1>
#else
  define list<frequency> H_offset=<$FQ1LIST>
#endif
#endif

/*******************************************************/
/* Assign cnsts to check validity of parameter range */
/*******************************************************/
#ifdef fsat
  "cnst10=plw10"          /* tsatpwr - set max at 0.00005W */
#endif

#ifdef mess_flg
  "cnst11=plw11"          /* tpwrmess pl11 - set max at 2.0W */
#endif

#ifdef Hsteady_flg
  "cnst13=spw13"          /* tpwrsl - set max at 0.001W" */
#endif

  "cnst14=spw14"          /* tpwrsl1 - set max at 0.001W" */
```

```
#ifdef c_flg
  "cnst22=spw22"         /* d_ad - set max at 57W */
#endif

#ifdef N_sel
  "cnst32=spw32"         /* power level for 15N selective pulse */
#endif

/*************************************************/
/* Set the weak H-amide B1 field for irradiation */
/*************************************************/
"p15=1000000.0/(4.0*cnst16)"
"plw15=plw1*(pwh)*(pwh)/((p15)*(p15))"
"cnst15=plw15"

/*****************************************************/
/* Set phase alignment and offset for shaped pulses  */
/*****************************************************/
"spoal13=0"
"spoal14=0"
"spoff13=0"
"spoff14=0"

/*****************************/
/* Initialize loop counters */
/*****************************/
"l2=0"
"l3=0"

"acqt0=0"
baseopt_echo

1 ze
/*************************************/
/* Check validity of parameter range  */
/*************************************/
#ifdef fsat
  if "cnst10 > 0.00005"
  {
    2u
    print "error: tsatpwr pl10 too large !!!  "
    goto HaltAcqu
  }
#endif

#ifdef mess_flg
  if "cnst11 > 2.0"
  {
    2u
    print "error:tpwrmess pl11 too large !!!  "
    goto HaltAcqu
  }
#endif

#ifdef Hsteady_flg
  if "cnst13 > 0.002"
  {
    2u
    print "error: tpwrsl spw13 too large !!!  "
    goto HaltAcqu
  }
#endif

  if "cnst14 > 0.002"
  {
    2u
    print "error: tpwrsl1 spw14 too large !!!  "
    goto HaltAcqu
  }

  if "cnst15 > 0.01"
  {
```

```
    2u
    print "error: cnst15 - power in W for 1H CEST is too large !!!  "
    goto HaltAcqu
  }

  if "cnst16 > 250"
  {
    2u
    print "error: cnst16 - weak 1H B1 field strength in Hz must be <= 250 Hz !!!  "
    goto HaltAcqu
  }

#ifdef c_flg
  if "cnst22 > 50"
  {
    2u
    print "error: d_ad spw22 is too large !!!  "
    goto HaltAcqu
  }
#endif

#ifdef N_sel
  if "cnst32 > 35"
  {
    2u
    print "error: spw23 is too large < 55W !!!  "
    goto HaltAcqu
  }
#endif

#if !defined(cal_HB1) && !defined(cal_HR1)
  if "time_T1 > 0.5s"
  {
    2u
    print "error: time_T1 is too long"
    goto HaltAcqu
  }
#endif

2 d11
/*****************************************/
/* Continue to check real time variables */
/*****************************************/
#ifdef cal_HB1
  "DELTA = time_cal[l2]"
  if "DELTA > 500m" {
    2u
    print "error: time_cal (evolution time during B1 calib is too long < 500 m"
    goto  HaltAcqu
  }
#endif

/*************************************************/
/*   Presaturation Period                        */
/*   option for Messrlie purge zgoptn -Dmess_flg   */
/*************************************************/
#ifdef mess_flg
  20u pl11:f1
  (dly_pg1 ph26):f1
  20u
  (dly_pg2 ph27):f1
  20u pl10:f1
#endif /*mess_flg*/

#ifdef fsat
  4u pl10:f1
  d1 cw:f1 ph26
  4u do:f1
  2u pl1:f1
#ifdef fscuba
  hscuba
  (pwh ph26):f1
  (pwh*2 ph27):f1
```

```
  (pwh ph26):f1
  hscuba
#endif /*fscuba*/
#else
  2u pl1:f1
  d1
#endif /*fsat*/

  20u UNBLKGRAD

/*************************************/
/* Erase 15N equilibrium magnetization */
/*************************************/
  2u pl3:f3
  (pwn ph26):f3

  2u
  p51:gp1
  d16

/*************************************************/
/*  +/- phase cycle on 1H prior to CEST period    */
/*************************************************/
#ifdef Hsteady_flg
  2u
  (pw_sl1:sp14 ph27):f1
  2u pl1:f1
  (pwh ph26 pwh*2 ph21 pwh ph26):f1
  (pw_sl:sp13 ph22):f1
  2u

  2u
  p51:gp1
  d16
#endif /*Hsteady_flg*/

/*************************************/
/*   CEST portion on Hz magnetization   */
/*************************************/
  2u pl15:f1
#ifdef cal_HB1
  "DELTA=time_cal[l2]"
  2u fq=cnst1:f1
  DELTA cw:f1 ph26
  2u do:f1
#else
#ifdef cal_HR1
  "DELTA=time_cal[l2]"
  DELTA
#else
  2u fq=H_offset:f1
  time_T1 cw:f1 ph26
  2u do:f1
#endif /*cal_HR1*/
#endif /*cal_HB1*/
  20u fq=0:f1 pl1:f1

  2u
  p52:gp2
  d16

/*********************************/
/*   TROSY-type H->N transfer     */
/*********************************/
  (pwn ph26):f3

  2u
  p53:gp3
  d16

  "DELTA = taua - 2u - p53 - d16"
  DELTA
```

```
  (center (pwh*2 ph26):f1 (pwn*2 ph26):f3)

  DELTA

  2u
  p53:gp3
  d16

  (pwn ph27):f3
  (pwh ph26):f1

  2u
  p54:gp4
  d16

#ifdef N_sel
  "DELTA = taua - 2u - p54 - d16 - pwn_sl*0.5"
#else
  "DELTA = taua - 2u - p54 - d16"
#endif
  DELTA

#ifdef N_sel
  (center (pwh*2 ph26):f1 (pwn_sl:sp32 ph26):f3)
#else
  (center (pwh*2 ph26):f1 (pwn*2 ph26):f3)
#endif

  DELTA

  2u
  p54:gp4
  d16

  (pwh ph27):f1

  /* shaped pulse */
  4u
  (pw_sl1:sp14 ph26):f1
  2u pl1:f1
  /* end shaped pulse */

  2u pl3:f3
  p55:gp5
  d16

/*********************/
/*   15N labeling    */
/*********************/
#ifndef Hsteady_flg
  (pwn ph1):f3
#else
  (pwn ph11):f3
#endif

  32u gron0*-1.0
  d0
  100u groff

#ifdef c_flg
  (center (pwh ph27 pwh*2.0 ph26 pwh ph27):f1 (pwc_ad:sp22 ph26):f2)
#else
  (pwh ph27 pwh*2.0 ph26 pwh ph27):f1
#endif

  32u gron0*1.0
  d0
  100u groff

/*********************************************/
/*   Encoding coherence selection gradient   */
/*********************************************/
  2u
```

```
  p56:gp6*-1.0
  d16

  "DELTA = BigT - 2u - p56 - d16"
  DELTA

  (pwn*2 ph2):f3

  2u
  p56:gp6*1.0
  d16

  "DELTA = BigT - 2u - p56 - d16 + 32u + 100u"
  DELTA

#ifdef c_flg
  (center (pwh ph27 pwh*2.0 ph26 pwh ph27):f1 (pwc_ad:sp22 ph26):f2)
#else
  (pwh ph27 pwh*2.0 ph26 pwh ph27):f1
#endif

  "DELTA = 32u + 100u"
  DELTA

/*****************************************/
/*   Planar mixing N->H back transfer    */
/*****************************************/
  (center (pwh ph28):f1 (pwn ph3):f3)

  2u
  p57:gp7
  d16

  "DELTA = taub - 2u - p57 - d16"
  DELTA

  (center (pwh*2 ph26):f1 (pwn*2 ph26):f3)

  DELTA

  2u
  p57:gp7
  d16

  (center (pwh ph27):f1 (pwn ph29):f3)

  2u
  p58:gp8
  d16

  "DELTA = taub - 2u - p58 - d16"
  DELTA

  (center (pwh*2 ph26):f1 (pwn*2 ph26):f3)

  DELTA

  2u
  p58:gp8
  d16

  if "l3%2 == 0" {
    (center (pwh ph26):f1 (pwn ph26):f3)
  }
  else {
    (center (pwh ph26):f1 (pwn ph28):f3)
  }

/*********************************************************/
/*   IPAP/S3E and decoding coherence selection gradient  */
/*********************************************************/
  2u
  p60:gp10*EA
```

```
  d16

  "DELTA = tauc - 2u - p60 - d16 - (pwn - pwh)*0.5"
  DELTA

#ifdef s3_flg
  (center (pwh*2 ph26):f1 (pwn*2 ph26):f3)
#else
  if "l3%2 == 0" {
    (center (pwh*2 ph26):f1 (pwn ph26 pwn ph28):f3)
  }
  else {
    (center (pwh*2 ph26):f1 (pwn*2 ph26):f3)
  }
#endif

#ifdef s3_flg
  "DELTA = tauc - 2u - p59 - d16 - 2u - p60 - d16 + pwh*2.0/PI - 4u - de - pwn*2"
#else
  "DELTA = tauc - 2u - p59 - d16 - 2u - p60 - d16 + pwh*2.0/PI - 4u - de"
#endif /*s3_flg*/
  DELTA

  2u
  p60:gp10*EA
  d16

  2u
  p59:gp9*EA
  d16

  4u BLKGRAD

#ifdef s3_flg
  if "l3%2 == 0" {
    (pwn ph26 pwn ph26):f3
  }
  else {
    (pwn ph26 pwn ph28):f3
  }
#endif

/***************************************/
/*   Test how much water left          */
/*   set d13=AQ and zgoptn -Dwater     */
/*   also use small value of rg        */
/***************************************/
#ifdef water
  if "nsdone == 0"
  {
    d13
    d1
    (pwh*0.1 ph26):f1
  }
  else
  {
    d13
  }
#endif

/***************************************/
/*   Signal detection and looping      */
/***************************************/
  if "l3%2 == 0" {
    go=2 ph30
  }
  else {
    go=2 ph31
  }
  d11 mc #0 to 2

  F3QF(calclc(l3,1))
#if defined(cal_HB1) || defined(cal_HR1)
```

```
  F2QF(calclc(l2,1))
#else
  F2QF(calclist(H_offset,1))
#endif /*cal_HB1, cal_HR1*/
  F1EA(calgrad(EA) & calph(ph3, +180), caldel(d0, +in0) & calph(ph1, +180) & calph(p
h11, +180) & calph(ph30, +180) & calph(ph31, +180))

HaltAcqu, 1m
exit

ph1=0 2 2 0
ph2=0 0 0 0 1 1 1 1 2 2 2 2 3 3 3 3
ph3=2
ph11=0 0 2 2
ph21=2 1
ph22=3 1
ph26=0
ph27=1
ph28=2
ph29=3
ph30=0 2 2 0 2 0 0 2
ph31=1 3 3 1 3 1 1 3

;d1 : Repetition delay d1
;d3 : taua ~1/4J(NH) 2.70 ms
;d5 : taub ~1/4J(NH) 2.70 ms
;d10 : internal delay
;d11 : disk read/write delay
;d12 : hscuba delay ~6ms
;d15 : BigT set to 850 us
;d16 : gradient recovery delay 200 us
;d17 : time_T1, time for CEST, typically several 100s of ms
;pl1 : tpwr - power level for 1H pulses
;pl3 : dhpwr2 -  power level for N hard pulses
;pl10 : tsatpwr - power level for water presat
;pl11 : tpwrmess - power level for Messerle purge
;p1 : pwh - 1H 90 degree pulse
;p3 : pwn - 15N 90 degree pulse
;p13 : pw_sl
;p14 : pw_sl1
;p22 : pwc_ad -  adiabatic C180 pulse width
;p32 : pwn_sl for selective pulse on amide N15s
;p51 : gradient pulse 51                                  [400 usec]
;p52 : gradient pulse 52                                  [1000 usec]
;p53 : gradient pulse 53                                  [500 usec]
;p54 : gradient pulse 54                                  [256 usec]
;p55 : gradient pulse 55                                  [1500 usec]
;p56 : gradient pulse 56                                  [625 usec]
;p57 : gradient pulse 57                                  [256 usec]
;p58 : gradient pulse 58                                  [256 usec]
;p59 : gradient pulse 59                                  [256 usec]
;p60 : gradient pulse 60                                  [400 usec]
;spw13 : tpwrsl - power level for water selective pulse pw_sl
;spw14 : tpwrsl1 - power level for water selective pulse pw_sl1
;spnam13 : shape for pw_sl
;spnam14 : shape for pw_sl1
;spnam22 : shape for pwc_ad
;spnam32 : shape for pwn_sl
;cnst1 : offset (Hz) for B1 calibration from o1
;cnst15 : power level for weak amide 1H B1 field
;cnst16 : weak CEST 1H B1 field in Hz
;l2 : pointer to the delay value for calibration of B1
;l3 : pointer to switch between IP and AP
;inf1 : 1/SW(X) = 2*DW(X)
;in0 : 1/(2*SW(x))=DW(X)
;nd0 : 2
;ns : 2*n
;FnMODE : echo-antiecho

;use gradient ratio:    gp 6 : gp 9
;                         80 : -39.5

;for z-only gradients:
```

```
;gpz0: 0.25%
;gpz1: -25%
;gpz2: 15%
;gpz3: -50%
;gpz4: 23%
;gpz5: -70%
;gpz6: 80%
;gpz7: 60%
;gpz8: 15%
;gpz9: -39.5%
;gpz10: 30%

;use gradient files:
;gpnam1: SMSQ10.32
;gpnam2: SMSQ10.32
;gpnam3: SMSQ10.32
;gpnam4: SMSQ10.32
;gpnam5: SMSQ10.32
;gpnam6: SMSQ10.32
;gpnam7: SMSQ10.32
;gpnam8: SMSQ10.32
;gpnam9: SMSQ10.32
;gpnam10: SMSQ10.32

;zgoptns : Df1180, Dc_flg, Dfsat, Dfscuba, Dc_flg, Dmess_flg, DN_sel, Dcal_HB1, Ds3_
flg, DHsteady_flg, Dcal_HR1
```